NAVAL POSTGRADUATE SCHOOL
Monterey, California

THESIS

VISUALIZATION OF THE FLOW FIELD AROUND AN OSCILLATING MODEL OF THE USS ENTERPRISE (CVN-65) IN A SIMULATED ATMOSPHERIC BOUNDARY LAYER

by

Thomas A. Cahill

March 1988

Thesis Advisor: J. Val Healey

REPORT DOCUMENTATION PAGE

1a REPORT SECURITY CLASSIFICATION UNCLASSIFIED	1b RESTRICTIVE MARKINGS
2a SECURITY CLASSIFICATION AUTHORITY	3 DISTRIBUTION / AVAILABILITY OF REPORT Approved for public release; distribution is unlimited
2b. DECLASSIFICATION / DOWNGRADING SCHEDULE	
4. PERFORMING ORGANIZATION REPORT NUMBER(S)	5 MONITORING ORGANIZATION REPORT NUMBER(S)
6a NAME OF PERFORMING ORGANIZATION Naval Postgraduate School 6b OFFICE SYMBOL (*If applicable*) Code 67	7a NAME OF MONITORING ORGANIZATION Naval Postgraduate School
6c. ADDRESS (*City, State, and ZIP Code*) Monterey, CA 93943-5000	7b. ADDRESS (*City, State, and ZIP Code*) Monterey, CA 93943-5000
8a. NAME OF FUNDING / SPONSORING ORGANIZATION 8b OFFICE SYMBOL (*If applicable*)	9 PROCUREMENT INSTRUMENT IDENTIFICATION NUMBER
8c. ADDRESS (*City, State, and ZIP Code*)	10. SOURCE OF FUNDING NUMBERS PROGRAM ELEMENT NO. / PROJECT NO / TASK NO / WORK UNIT ACCESSION NO

11. TITLE (*Include Security Classification*)
VISUALIZATION OF THE FLOW FIELD AROUND AN OSCILLATING MODEL OF THE USS ENTERPRISE (CVN-65) IN A SIMULATED ATMOSPHERIC BOUNDARY LAYER

12. PERSONAL AUTHOR(S)
Cahill, Thomas A.

13a. TYPE OF REPORT	13b TIME COVERED	14. DATE OF REPORT (*Year, Month, Day*)	15 PAGE COUNT
Master's Thesis	FROM _____ TO _____	1988, March	90

16 SUPPLEMENTARY NOTATION
The views expressed in this thesis are those of the author and do not reflect the official policy or position of the Department of Defense or the U.S. Govt.

17. COSATI CODES			18 SUBJECT TERMS (*Continue on reverse if necessary and identify by block number*)
FIELD	GROUP	SUB-GROUP	Flow Visualization; Aircraft Carrier; Atmospheric Boundary Layer; Ship Motion Simulation

19 ABSTRACT (*Continue on reverse if necessary and identify by block number*)

A flow visualization study of an oscillating, 1:350 scale model of the USS Enterprise (CVN-65) was conducted in a low speed wind tunnel, modified to simulate an open ocean atmospheric boundary layer. The theories, equipment and techniques employed in this study are explained in detail and an analysis of the photographic results is included in this report. Both the helium bubble and fluorescent minituft methods of flow visualization yielded excellent results and recommendations for follow-on studies are suggested.

20 DISTRIBUTION / AVAILABILITY OF ABSTRACT ☒ UNCLASSIFIED/UNLIMITED ☐ SAME AS RPT ☐ DTIC USERS	21. ABSTRACT SECURITY CLASSIFICATION Unclassified
22a. NAME OF RESPONSIBLE INDIVIDUAL Prof. J. Val Healey	22b TELEPHONE (*Include Area Code*) (408) 646-2804 22c. OFFICE SYMBOL Code 67He

DD FORM 1473, 84 MAR 83 APR edition may be used until exhausted
All other editions are obsolete

SECURITY CLASSIFICATION OF THIS PAGE
☆ U.S. Government Printing Office: 1986—606-24.
UNCLASSIFIED

Approved for public release; distribution is unlimited

Visualization of the Flow Field Around an Oscillating Model of the USS Enterprise (CVN-65) in a Simulated Atmospheric Boundary Layer

by

Thomas A. Cahill
Lieutenant Commander, United States Navy
B.S., U.S. Naval Academy, 1976

Submitted in partial fulfillment of the
requirements for the degree of

MASTER OF SCIENCE IN AERONAUTICAL ENGINEERING

from the

NAVAL POSTGRADUATE SCHOOL
March 1988

ABSTRACT

A flow visualization study of an oscillating, 1:350 scale model of the USS Enterprise (CVN-65) was conducted in a low speed wind tunnel, modified to simulate an open ocean atmospheric boundary layer. The theories, equipment and techniques employed in this study are explained in detail and an analysis of the photographic results is included in this report. Both the helium bubble and fluorescent minituft methods of flow visualization yielded excellent results and recommendations for follow-on studies are suggested.

TABLE OF CONTENTS

I. INTRODUCTION ---------- 1

II. EXPERIMENTAL SIMULATION AND APPARATUS ---------- 5

A. MODELING THE ATMOSPHERIC BOUNDARY LAYER ----- 6

1. Theoretical Considerations ---------- 6

2. Experimental Simulation ---------- 8

3. Wind Tunnel and Modifications ---------- 9

4. Effect of Modifications ---------- 12

B. SHIP MOTION SIMULATION ---------- 15

1. Theoretical Considerations ---------- 15

2. Experimental Simulation ---------- 17

3. Oscillating Mechanism ---------- 19

4. The Ship Model ---------- 22

III. FLOW VISUALIZATION TECHNIQUES ---------- 27

A. OFF-BODY TECHNIQUE ---------- 27

1. Helium Bubble System ---------- 27

2. Lighting and Photography ---------- 30

B. ON-BODY TECHNIQUE ---------- 34

1. Fluorescent Minitufts ---------- 34

2. Lighting and Photography ---------- 36

IV. RESULTS AND DISCUSSION ---------- 40

A. SCOPE OF INVESTIGATION ---------- 40

B. ZERO DEGREE YAW ---------- 43

C. TWELVE DEGREE STARBOARD YAW ---------- 45

V. CONCLUSIONS AND RECOMMENDATIONS ---------- 72

A. HELIUM BUBBLE FLOW VISUALIZATION ---------- 72

B. FLUORESCENT MINITUFT TECHNIQUE ---------- 73

C. THESIS TOPIC SUGGESTION ---------- 74

LIST OF REFERENCES ---------- 76

INITIAL DISTRIBUTION LIST ---------- 78

LIST OF TABLES

1. TEST SECTION VELOCITY DATA (FT/SEC) ---------- 11

2. TEST SECTION % TURBULENCE INTENSITY DATA ---------- 13

3. SHIP MOTION PARAMETERS ---------- 19

LIST OF FIGURES

1. NPS Flow Visualization Tunnel ---------- 14
2. Ship Model Oscillating Mechanism ---------- 23
3. Diagram of the USS Enterprise (CVN-65) ---------- 24
4. Diagram of the Helium Bubble System ---------- 28
5. Diagram of CV Flight Deck ---------- 42
6. Forward: 0^{o} Yaw, 0^{o} Pitch, 0^{o} Roll ---------- 46
7. Aft: 0^{o} Yaw, 0^{o} Pitch, 0^{o} Roll ---------- 47
8. Forward: 0^{o} Yaw, 1.25^{o} Up Pitch, 0^{o} Roll -------- 48
9. Aft: 0^{o} Yaw, 1.25^{o} Up Pitch, 0^{o} Roll ---------- 49
10. Forward: 0^{o} Yaw, 1.25^{o} Down Pitch, 0^{o} Roll ------ 50
11. Aft: 0^{o} Yaw, 1.25^{o} Down Pitch, 0^{o} Roll ---------- 51
12. Forward: 0^{o} Yaw, 0^{o} Pitch, 6^{o} Port Roll --------- 52
13. Aft: 0^{o} Yaw, 0^{o} Pitch, 6^{o} Port Roll ---------- 53
14. Forward: 0^{o} Yaw, 0^{o} Pitch, 6^{o} Starboard Roll ---- 54
15. Aft: 0^{o} Yaw, 0^{o} Pitch, 6^{o} Starboard Roll -------- 55
16. Forward: 0^{o} Yaw, Oscillating Pitch and Roll ----- 56
17. Aft: 0^{o} Yaw, Oscillating Pitch and Roll --------- 57
18. Forward: 12^{o} Yaw, 0^{o} Pitch, 0^{o} Roll ---------- 60
19. Aft: 12^{o} Yaw, 0^{o} Pitch, 0^{o} Roll ---------- 61
20. Forward: 12^{o} Yaw, 1.25^{o} Up Pitch, 0^{o} Roll ------- 62
21. Aft: 12^{o} Yaw, 1.25^{o} Up Pitch, 0^{o} Roll ---------- 63
22. Forward: 12^{o} Yaw, 1.25^{o} Down Pitch, 0^{o} Roll ----- 64
23. Aft: 12^{o} Yaw, 1.25^{o} Down Pitch, 0^{o} Roll --------- 65

24. Forward: 12° Yaw, 0° Pitch, 6° Port Roll -------- 66
25. Aft: 12° Yaw, 0° Pitch, 6° Port Roll ---------- 67
26. Forward: 12° Yaw, 0° Pitch, 6° Starboard Roll --- 68
27. Aft: 12° Yaw, 0° Pitch, 6° Starboard Roll ------- 69
28. Forward: 12° Yaw, Oscillating Pitch and Roll ---- 70
29. Aft: 12° Yaw, Oscillating Pitch and Roll -------- 71

ACKNOWLEDGEMENTS

Many thanks to Dr. Healey for his insight and encouragement that helped me to overcome obstacles. Special thanks are due to John Moulton and Ron Ramaker, Aero Department Technicians. I'm grateful for the prompt assistance provided by Ms. Dale Ward, Mr. Mitch Nichols and Mr. Andy Sarakon of the NPS Photo Lab.

My deepest gratitude is extended to Janie, Jeannie and Andrew for their love and support, and to the Lord for his many blessings.

I. INTRODUCTION

Air vehicles of all types currently operate from the decks of U. S. Navy ships and are subject to the hazards of superstructure wake turbulence and ship motion during take off and landing operations. Conventional and V/STOL fixed wing aircraft, helicopters, remotely piloted vehicles and tethered aerostats are either in service in fleet units or are contemplated for future, wide-spread employment. Additionally, the variety of missile systems currently employed in most fleet units must also contend with superstructure wake turbulence and ship motion in the relatively low speed boost phase of launch. In light of these developments, an understanding of the interaction between the atmospheric boundary layer, the ship's above-the-water-line geometry, the ship's motion and the turbulence generated by the air vehicle is appropriate.

Of immediate concern to the Navy is the determination of the safe operating envelopes of ship/helicopter pairs. The Naval Air Test Center defines the envelopes by exercising ships and helicopters at sea at a cost of between $75,000 and $150,000 per combination, as assets are made available from the operational force. Understandably, there is a backlog involving 20 classes of ships and 11 helicopter types, as reported by Carico, McCallum and Higman [Ref. 1].

This backlog is all the more significant when one considers that each landing spot on a given ship must be certified. The number of safe operating envelopes that need to be defined may range from one to nine, one for each spot, depending on ship type. The high cost and infrequent availability of assets has generated interest in the possibility of defining operating envelopes through simulation. Simulation has the additional advantage of examining operating envelopes in varying sea states and wind conditions, an advantage that cannot be duplicated in a timely manner at sea with ship/helicopter pairs. While extensive work has been conducted in the fields of ship motion prediction and helicopter turbulence modeling, ship air wake analysis is an underdeveloped field of study.

This report investigates the air wake turbulence of a 1:350 scale model of the USS Enterprise (CVN-65) by flow visualization in support of the larger, long range effort to establish a facility at the Naval Postgraduate School that accurately simulates the ship/helicopter interface and that is equipped to extract the mean velocity, turbulence intensity and spectrum function from ship air wakes.

Interest in air wake studies, motivated by the need to understand their impact on flight performance, is not new. Healey [Ref. 2:pp. 14-16] summarizes the results of two decades of effort in this field. Missing from previous air wake studies was due consideration of the significant impact

that shear flow and free stream turbulence has on the overall turbulence of the air wake. No attempt was made in previous reports to model the earth's atmosphere, which is essentially a sheared, turbulent boundary layer. In previous studies, models were exposed to uniform flows that had turbulence levels of about one-half percent. In reality, free stream turbulence levels of between ten and 18 percent are more common, the result of wind and rough seas. Additionally, the potential that complex interactions may exist between free stream flows and moving ships has not been fully explored. Incorporation of the results of previous air wake studies into helicopter flight simulators that simulate the ship environment, has not resulted in improved modeling of actual conditions [Ref. 2:pp.56-58]. In one case, which involved the ship/helicopter interface between a DD-963 class destroyer and a SH-2F Sea Sprite, the standard deviation and frequency content of the air wakes were found to be excessive and a characteristic far field air disturbance was absent [Ref. 3].

With these deficiencies in mind, the initial phases of the ongoing research being conducted at the Naval Postgraduate School dealt with the modeling of the atmospheric boundary layer in an existing low speed wind tunnel followed by the design and installation of a ship motion simulator in the tunnel. In the past, generic, 1:170 scale, block models simulating destroyer type ships have

been installed in the tunnel to refine flow visualization techniques. These phases will be reviewed in this paper, followed by descriptions of the ship model and flow visualization techniques employed to obtain the results, conclusions and recommendations submitted at the end of this report.

II. EXPERIMENTAL SIMULATION AND APPARATUS

Rae and Pope [Ref. 4:p. 484] describe five parameters that must be considered in order to conduct testing in a wind tunnel that simulates the atmospheric boundary layer. As related to this investigation of a ship's air wake, these parameters are:

1. Matching Rossby numbers.
2. Matching the zero pressure gradient found in the real world.
3. Kinematic simulation of the air flow, boundary layer, velocity distribution and turbulence.
4. Maintaining Reynolds number of about 50,000 so as to achieve viscous/inertial similarity between the model and the full scale ship.
5. Proper scaling of the ship; proper simulation of ship motion by maintaining a constant Strouhal number.

The Rossby number is concerned with the effect of the rotation of the earth on its winds. For the sake of simplicity, an idealized neutral density atmospheric boundary layer, such as is associated with a stationary air mass, is assumed. Coriolis forces are considered to be negligible, therefore the Rossby number is ignored.

A longitudinal pressure gradient is normally present in a wind tunnel and is aggravated by a thick boundary layer. The influence of this gradient is assumed to be negligible because the tunnel employed is operated at a low velocity,

consistent with the need to maintain the minimum Reynolds number discussed above.

The manner in which the remaining requirements were met in order to obtain a faithful simulation, will be discussed in detail.

A. MODELING THE ATMOSPHERIC BOUNDARY LAYER

From the outset, it must be recognized that the atmospheric boundary layer is a dynamic environment. Frequent changes in wind velocity, sea state and meteorological conditions are characteristic, whether a ship is stationary or moving between differing bodies of water. Additionally, the accuracy of recorded meteorological and oceanographic data on which any simulation is based, is suspect. For instance, the accuracy of a ship's anemometer, used to measure relative wind speed and direction, is known to be influenced by its location on the superstructure and is susceptible to air wake interference. Nonetheless, approaches to atmospheric boundary layer simulation exist. The best source for information concerning this field is in the Journal of Wind Engineering and Industrial Aerodynamics.

1. Theoretical Considerations

There are four parameters which significantly affect the characteristics of the free stream air flow. Healey [Ref. 2:pp. 4-5] identifies them as:

a. The mean speed, U, which is an average of the observed wind speed over an arbitrary period of time.

b. The turbulence intensity, which is the standard deviation, σ, of the longitudinal wind speed fluctuations about the mean speed divided by the mean speed.

c. The longitudinal scale length of the turbulence, L, which is the mean length of the most energetic eddies in the turbulence.

d. The spectrum function of the turbulence, which indicates the frequency and amplitude distribution of the turbulent energy.

These last three parameters can be described by empirical relationships that are functions of:

a. The elevation, Z (meters), above a given surface.

b. The mean wind speed, U(Z) (meters/sec), as a function of elevation.

c. The roughness length scale, z_o (meters), a measure of ground roughness that is not related to ground obstacle height. Davenport [Ref. 5] gives rough sea values of z_o that range from 0.001 to 0.01 meters.

The mean wind speed, U(Z), and the elevation, Z, are selected on the basis of what wind speed and flight deck elevation one wishes to simulate and they are the independent variables that enter into the determination of the roughness length scale, z_o. Garratt [Ref. 6] relates the drag coefficient for the neutral air flow over the sea and the Monin-Obukov similarity theory by developing the following equation:

$$z_o = Z\exp\{-0.41/[(0.067U(Z)+0.75)x10^{-3}]^{1/2}\} \qquad (1)$$

where the radical term is the drag coefficient and 0.41 is the Von Karman constant. With Z and z_o known, ESDU data

item 74031 [Ref. 7] can be entered to obtain the characteristic turbulence intensity.

The longitudinal scale length of the turbulence, L, in and of itself, is not significant, however the ratio of the length scale to the beam of the ship is important. The higher the ratio is, the more the flow field behaves like a time dependant , non-random phenomena. With z_o calculated, ESDU 74031 [Ref. 7] can be again employed to obtain the scale length parameter.

The final free stream air flow parameter, the spectrum function of the atmospheric boundary layer, has been modeled by Dryden, Kaimal and Von Karman, the later being the most frequently used function:

$$S(n) = 4L\ \sigma^2/\{U[1.0+70.8\tilde{n}^2]^{5/6}\} \qquad (2)$$

where **n** is the frequency (Hz) and $\tilde{n}$ = nL/U, variables that have been previously defined.

2. Experimental Simulation

During the initial stages of research at the Naval Postgraduate School, attention focused on the severe flight deck motion and the highly turbulent air wake faced by helicopter pilots operating from destroyer type ships in conditions of rough seas and high winds. At a mean flight deck elevation of **Z** = 10 meters, a maximum mean wind velocity of about 50 knots (**U(Z)** = 25 m/s) was postulated

[Ref. 2:p.11]. A roughness length scale, z_o, of 0.0024 meters results from Equation (1). ESDU 74031 [Ref. 7] yields a turbulence intensity of 0.14 and a longitudinal scale length of $65 < L < 75$ meters, which in turn results in a ratio to the beam of the typical destroyer (17 meters) of about four.

A boundary layer can be structured by using the above information and the following commonly known expression which Rae and Pope [Ref. 4:p.491] provide:

$$U/U_{ref} = (Z/Z_{ref})^{\alpha} \qquad (3)$$

where, in this initial investigation, U_{ref} = 25 m/s, Z_{ref} = 10 meters and α is the boundary layer shape coefficient. Davenport [Ref. 5] provides values of α that range from 0.11 to 0.15. Also provided is the approximate thickness of the atmospheric boundary layer above the sea, 250 meters.

Simulating the above boundary layer and turbulence intensity level in an existing low speed wind tunnel at the Naval Postgraduate School, was accomplished and described in detail by Bolinger [Ref. 8:pp. 18-28] and is reviewed below.

3. Wind Tunnel and Modifications

a. Wind Tunnel Description

The wind tunnel employed in this research was an existing low speed "smoke" or flow visualization tunnel. The tunnel is of the open circuit type and it draws air into

the test section through a 15 square foot intake that is covered over with three inches of honeycomb and screening material. The intake contracts to a five square foot test section, 22 feet in length. Mounted on the walls of the test section are plexiglass windows for viewing, lighting and photography; elsewhere the walls are painted with flat black paint to reduce glare. Once through the test section, the air passes through louvers and a circular duct to a five foot diameter, sixteen blade, variable pitch fan that is powered by a constant speed AC motor. Velocities ranging from near zero to 11 m/s are possible. At this point, the air is exhausted to the outdoors.

b. Wind Tunnel Modifications

Employing a variation of Counihan's research [Ref. 9], Bolinger [Ref. 8:p. 18] introduced into the tunnel four 30 inch high vortex generators and three 30 inch high cones with a base diameter of two inches. A target velocity of 2.0 m/s, approximately 6.56 ft/s, at an elevation of about two inches from the tunnel floor, the minimum height of the typical flight deck on a given ship model, was sought. This velocity, coupled with the typical model beam width of six to eight inches, yields the needed Reynolds number of around 50,000 that was previously discussed. Subsequent velocity profile measurements, taken by means of a single wire probe and DANTEC hot wire apparatus, yielded the results summarized in Table 1 and a statistically

TABLE 1

TEST SECTION VELOCITY DATA (FT/S)
[REF. 8: P. 22]

	Z- Height above floor (inches)								
X*	2.00	3.00	4.00	8.00	12.00	16.00	19.00	25.00	30.00
6.00	6.21	6.36	6.63	7.81	7.84	8.13	8.44	8.61	9.15
9.00	6.32	6.35	6.84	7.89	7.78	8.00	8.40	8.60	9.23
12.00	6.24	6.40	6.88	7.83	7.80	8.09	8.37	8.65	9.16
15.00	6.29	6.39	6.78	7.65	7.88	8.25	8.40	8.65	9.21
18.00	6.23	6.41	6.58	7.53	7.90	8.17	8.41	8.43	9.07
21.00	6.34	6.43	6.70	7.80	8.05	8.16	8.53	8.59	9.27
24.00	6.30	6.13	6.74	7.79	8.01	8.09	8.49	8.51	9.24
27.00	6.28	6.26	6.85	7.77	7.96	8.05	8.41	8.60	9.01
30.00	6.24	6.22	6.77	7.85	7.89	8.01	8.28	8.58	9.21
33.00	6.22	6.30	6.65	7.79	7.84	7.98	8.38	8.56	8.96
36.00	6.31	6.10	6.71	7.56	7.78	8.06	8.43	8.64	8.91
39.00	6.29	6.17	6.74	7.66	7.80	8.09	8.44	8.59	9.21
42.00	6.26	6.20	6.72	7.76	7.82	8.07	8.34	8.57	8.98
45.00	6.33	6.37	6.83	7.76	7.85	8.06	8.34	8.63	9.03
48.00	6.25	6.34	6.73	7.84	7.95	8.27	8.38	8.64	8.83
51.00	6.25	6.27	6.79	7.77	8.01	8.24	8.44	8.77	9.08
AVE.	6.27	6.29	6.75	7.75	7.89	8.11	8.41	8.60	9.10
V/Vo	0.68	0.69	0.74	0.85	0.87	0.89	0.92	0.95	1.00
SIGMA	0.04	0.09	0.08	0.09	0.08	0.08	0.06	0.07	0.13

Vo at 30 inches = 9.1 ft/sec
* transverse position from far wall in inches

determined boundary layer shape coefficient, α, of 0.139, well within the range previously reported.

To increase the turbulence of the flow, various lengths, ranging from one to six inches, of 3/8 inch diameter dowels were randomly placed across the width of the tunnel floor to a depth of 18 inches forward of the test section. Table 2 summarizes the turbulence intensities that were computed. The average turbulence intensity of 0.12 present in the tunnel area of interest, from the floor to an elevation of eight inches, is within the 0.11 to 0.18 range discussed in Chapter I and the distribution of data compares favorably with ESDU information [Ref. 8:p. 27].

A pitot static probe permanently mounted to the tunnel ceiling and connected to an EDM 2500C micromanometer, is available to periodically check that the velocity above the boundary layer is around 9.1 ft/s, thereby insuring that the velocity profile and turbulence levels are faithfully reproduced. The above mentioned modifications are depicted in Figure 1.

4. Effect of Modifications

A discussion on how the results reported by Bolinger [Ref. 8] influence the conduct of this current investigation is appropriate because of the dimensional differences between a destroyer and an aircraft carrier. Of particular note is the carrier's mean flight deck elevation, Z, of 18.29 meters (60 feet). ESDU data [Ref. 7] yield a

TABLE 2

TEST SECTION % TURBULENCE INTENSITY DATA
[REF. 8: P. 26]

	Z- Height above floor (inches)								
X*	2.00	3.00	4.00	8.00	12.00	16.00	19.00	25.00	30.00
6.00	11.57	12.22	13.73	3.80	3.90	3.80	3.00	3.10	1.90
9.00	11.34	11.21	11.80	3.81	3.80	3.40	2.80	2.90	1.20
12.00	12.39	13.70	11.67	3.73	3.60	3.70	3.20	2.90	1.60
15.00	12.83	12.79	10.05	4.09	3.70	3.60	3.10	3.30	1.80
18.00	12.25	13.41	11.34	4.06	4.20	4.20	3.30	4.10	3.00
21.00	11.00	13.83	8.90	5.20	3.80	3.80	3.60	2.90	2.11
24.00	11.27	12.70	12.78	6.07	4.00	3.80	3.50	3.70	1.80
27.00	11.21	10.84	10.16	5.59	3.80	3.60	3.50	3.10	2.40
30.00	11.68	12.72	11.71	4.53	3.77	3.40	2.90	2.80	1.90
33.00	11.77	11.03	11.07	5.05	3.90	3.60	2.70	2.80	2.50
36.00	11.41	11.58	9.38	6.21	4.30	3.60	3.20	3.30	2.70
39.00	12.26	11.33	9.58	5.55	4.50	3.90	3.40	3.60	2.30
42.00	12.74	12.09	12.75	4.70	3.80	3.67	3.30	3.40	2.80
45.00	12.09	12.11	10.96	4.80	3.90	3.50	3.60	3.20	2.50
48.00	12.47	12.76	12.48	4.70	3.80	3.60	2.90	2.70	2.40
53.00	11.26	12.67	12.98	4.80	4.00	3.50	3.90	3.10	2.20
AVE.	11.85	12.32	11.33	4.79	3.92	3.66	3.24	3.18	2.19
SIGMA	0.56	0.90	1.37	0.76	0.22	0.19	0.33	0.37	0.47

Vo at 30 inches = 9.1 ft/sec
* transverse position from far wall in inches

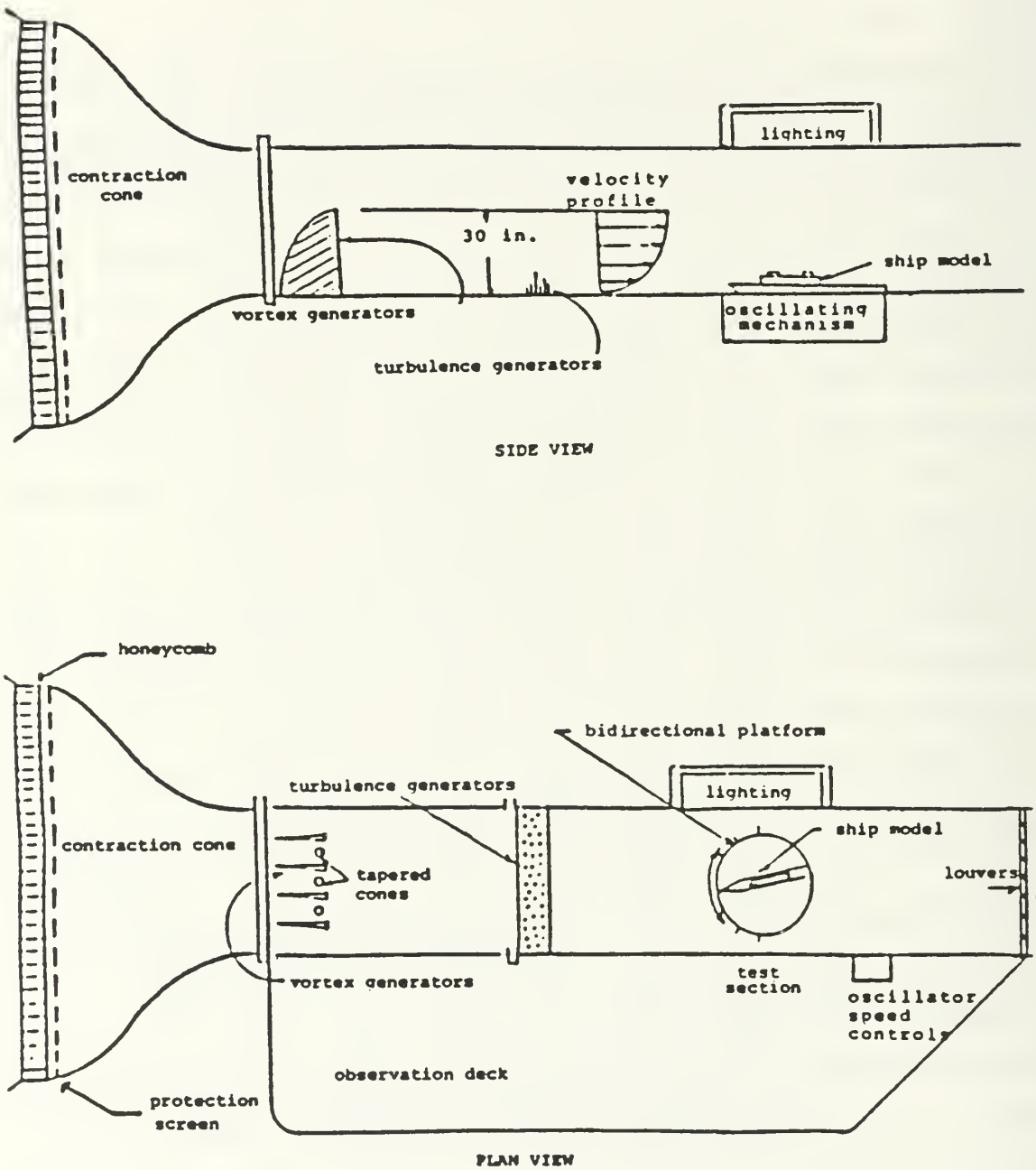

Figure 1. NPS Flow Visualization Tunnel [Ref. 10:p. 20]

longitudinal length scale of 80 < **L** < 90 meters, a function of this **Z** and 0.001 < z_o < 0.01 meters. The ratio of **L** to the carrier's beam (78.3 meters) equals 1.1, less than the ratio for the destroyer, thereby indicating that the flow field around an aircraft carrier is relatively less time dependent and more random than that of a destroyer. For this **Z** and for the average tunnel turbulence intensity of 0.12 previously reported, z_o = 0.0013 as determined from ESDU data [Ref. 7]. Working equation (1) so as to solve for **U(Z)** results in **U(Z)** = 16 m/s or just over 31 knots. This natural wind speed, as opposed to ship generated "wind over the deck," roughly corresponds to Sea State 5 (8-13 foot wave height) of the World Meteorological Organization code [Ref. 11:p. 1059]. This information impacts on the conduct of the ship motion simulation and the Strouhal number matching, two of the topics to be covered in the next section.

B. SHIP MOTION SIMULATION

1. Theoretical Considerations

The interaction between sea waves and a ship is a complex, nonlinear relationship. By treating ship motion as a six degree of freedom spring-mass-damper model and by making other assumptions, the David W. Taylor Naval Ship Research and Development Center (DTNSRDC) developed a state-of-the-art Ship Motion Program (SMP) that predicts the motion of a ship given its hull geometry, mass distribution,

its speed and heading, and the sea state. Healey [Ref. 2: p. 30] reported that the principal assumptions in the SMP are:

a. Monohull ship assumed.

b. Strip theory applicable.

c. Linearized equations are utilized; the dominant nonlinear behavior of roll is accounted for by modification to the roll damping coefficient.

d. Response Amplitude Operators can be obtained from wave and ship motion harmonics.

e. The three translational modes of motion (heave, sway and surge) are uncoupled from the rotational modes (roll, pitch and yaw).

Predictions are based on the product of a ship's Response Amplitude Operators, the sea spectra and the frequency mapping [Ref. 12:p. 5]. A Response Amplitude Operator (RAO) is a dimensional scaling factor between the wave's encounter energy and the ship's response energy at a given frequency. RAO's describe the six degree of freedom response to regular sinusoidal waves of unit amplitude. RAO's are required for irregular sea computations which determine ship responses to various seaways defined by sea spectra of unit significant wave height and a range of modal wave periods [Ref. 12: p. 27]. Irregular seas are usually categorized as either long or short crested. Long crested waves usually originate at great distances and form parallel lines, while short crested waves have a dominant direction but have a brief duration. Irregular sea predictions are sought for ship motion

modeling and they are provided in the form of Response Statistical Values, an output of the SMP.

The authors of the SMP have reported good agreement of computer generated data with tow tank model tests, most recently in 1985 [Ref. 13].

To summarize, given the ship type, the range of ship speed and the sea state one wishes to prescribe, the SMP can predict the full range of ship motion. Information provided by the program includes significant values of the pitch and roll angles, the respective pitch and roll sea encounter periods and the reference locations on the ship's hull from which the modes of motion act. The term "significant value" is defined as the average of the highest amplitudes observed during one-third of a given time period. The "sea encounter period" is the peak period of the response encounter spectra and is a close approximations to the period of extreme motion cycles of a ship in irregular seas [Ref. 12:p. 16].

2. Experimental Simulation

Conversation with one of the authors of the SMP, Mr. Terry Applebee, yielded the information on which to base the ship motion simulation. For sea state 5 (8-13 foot wave height) and for aircraft carrier speeds ranging from 0 to 35 knots, the significant values of the roll angle varied from 1.5^{o} to 11.4^{o} respectively. The sea encounter period for roll ranged from 22 to 24 seconds. In a like manner, the significant values of the pitch angle for the same speed

range were from 0.7^{o} to 1.3^{o} and the sea encounter period ranged from 10 to 15 seconds. The reference point from which the roll angle was taken to act was at the water line, while the reference point for the pitch angle was located at the water line, 55% of the distance between the bow and the stern. Mindful of the need to simulate realistic conditions, but also of the need to significantly alter the profile of the model to the free stream wind in the tunnel so as to detect changes to the flow field, a roll angle of 6^{o} and a pitch angle of 1.25^{o} became the motion characteristics to be employed in the ship motion simulation. The sea encounter periods were 24 and 10 seconds respectively. These responses are predicted to be typical for an aircraft carrier speed of 20 knots encountering eight foot high, long crested waves.

The introduction of motion to the ship air wake simulation necessitates the employment of the Strouhal number. The Strouhal number is a dimensionless quantity defined as follows:

$$\text{Strouhal number} = nL/U \qquad (4)$$

where **n**, the frequency of the oscillation, equals the inverse of the sea encounter period, **L** is the characteristic length, in this case the ship's beam, and **U** is the wind speed. For accurate modeling, a constant Strouhal number

must be maintained between the model and the full scale ship. Since the dimensional scale is fixed and the velocity profile of the simulated atmospheric boundary layer is constant, the model oscillating frequency remains as the dependent variable. Table 3 outlines this relationship and presents the frequencies at which the ship model must be oscillated to obtain similarity of results.

TABLE 3

SHIP MOTION PARAMETERS

Variable	Full Scale	Model
L	78.3 m	0.224 m
U	16.0 m/s	1.91 m/s
n (pitch)	0.1 Hz	4.18 Hz
n (roll)	0.042 Hz	1.74 Hz

3. Oscillating Mechanism

A system that produces roll and pitch (or heave) motion was installed by Biskaduros [Ref. 10] in the NPS flow visualization wind tunnel in November 1987. A 44 inch diameter hole was cut out of the floor of the wind tunnel, centered in front of the test section viewing window. A mounting frame was installed below the hole to which was attached the oscillating mechanism. The design of the mechanism called for independent pitch (or heave) and roll

motion systems so as to allow the investigation of either linearly uncoupled or nonlinear, coupled motion effects.

To simulate longitudinal motion, a five ampere, one-half horsepower Minarik motor turns a shaft by means of a belt drive. Attached at each end of the shaft are flanges, to which are installed eccentric pins that may be adjusted along the radius of the flange. Depending on the relationship between the angular position of the pins, pitch, heave or a combination of pitch and heave, can be obtained. Since pitch is the significant mode of longitudinal motion, one that can be observed and measured at sea, it is simulated in this investigation and heave is disregarded. The rotational motion of the flanges and the eccentric pins is transformed into vertical displacement by means of a "Scotch yoke" device, one at each flange. The eccentric pin rides in the slot of the yoke; if the pin is displaced from the flange center, the yoke completes one up/down cycle in one revolution of the flange. The yokes are held in the vertical orientation by Teflon guides. The model is attached to the top the yokes. The control box for the motor is located at the observation deck in the tunnel. Once power is applied, a control knob is used to adjust the RPM. At full speed, with a model mounted, 210 RPM or 3.5 Hz is the maximum obtainable pitch oscillation, as measured by a Monarch Instruments TACH IV electronic tachometer. To set a desired pitch angle, one can determine how many tenths of

an inch the eccentric pins need to be displaced from center by making a simple trigonometric calculation. The setting can be further refined by using a Watts precision clinometer. Pitch angles ranging from 0^{o} to 5^{o} can be set on the mechanism.

Roll motion is achieved by means of direct connection between an eccentric pin, mounted to a flange that is directly rotated by a one ampere, one-eighth horsepower Bodine motor, and a pin mounted to the bottom of the model's hull. The range of roll angles that can be obtained is between 0^{o} and 10^{o}; the distance between the flange and the model hull is the limiting factor that determines the maximum roll angle. At full power and with a model mounted, the Bodine motor achieves 130 RPM, therefore a roll oscillation of 2.15 Hz is obtainable.

The oscillating mechanism can be rotated through 360^{o} on its frame. To cover the hole in the tunnel floor, a customized disk must be manufactured for each model. Cut out of the center of a 44 inch diameter, 3/4 inch thick plywood disk, is the hull form of the model as measured at the water line. An additional 1/2 inch of wood is removed around the cut out to allow the application of weather stripping, a double layer of self-adhesive foam covered with three inch wide clear tape, to achieve an air tight seal between the oscillating model hull and the underside of tunnel floor. The disk is flush with the inside tunnel

floor and is tight fitting so as to inhibit outside air leakage. The disk is free to rotate, like a turntable, with the oscillating mechanism when different model yaw settings are desired. This system is depicted in Figure 2.

4. The Ship Model

Scale models available from government sources are either too large for the NPS flow visualization wind tunnel test section or, if the appropriate size (about 40-48 inches in length), are not available or suitable for modification that adapts them to the oscillating mechanism or for the flow visualization techniques. Custom-made models cost anywhere from $700 commercially to $20,000-$50,000 from government shops. The fidelity of the reproduction naturally varies with the price.

In the interim, while overseas sources are being explored, two 1:350 scale model kits of the USS Enterprise (CVN-65), manufactured by the Tamiya Plastic Model Company of Japan, have been procured from commercial sources at a cost of about $160 each. The significant dimensions of the model are listed below:

* Length: 40 inches
* Maximum width: 9.25 inches
* Flight deck height (from water line): 2.75 inches
* Superstructure height (from water line): 7 inches

Figure 3 depicts this aircraft carrier's profile. While it is recognized that this model might be inappropriate for

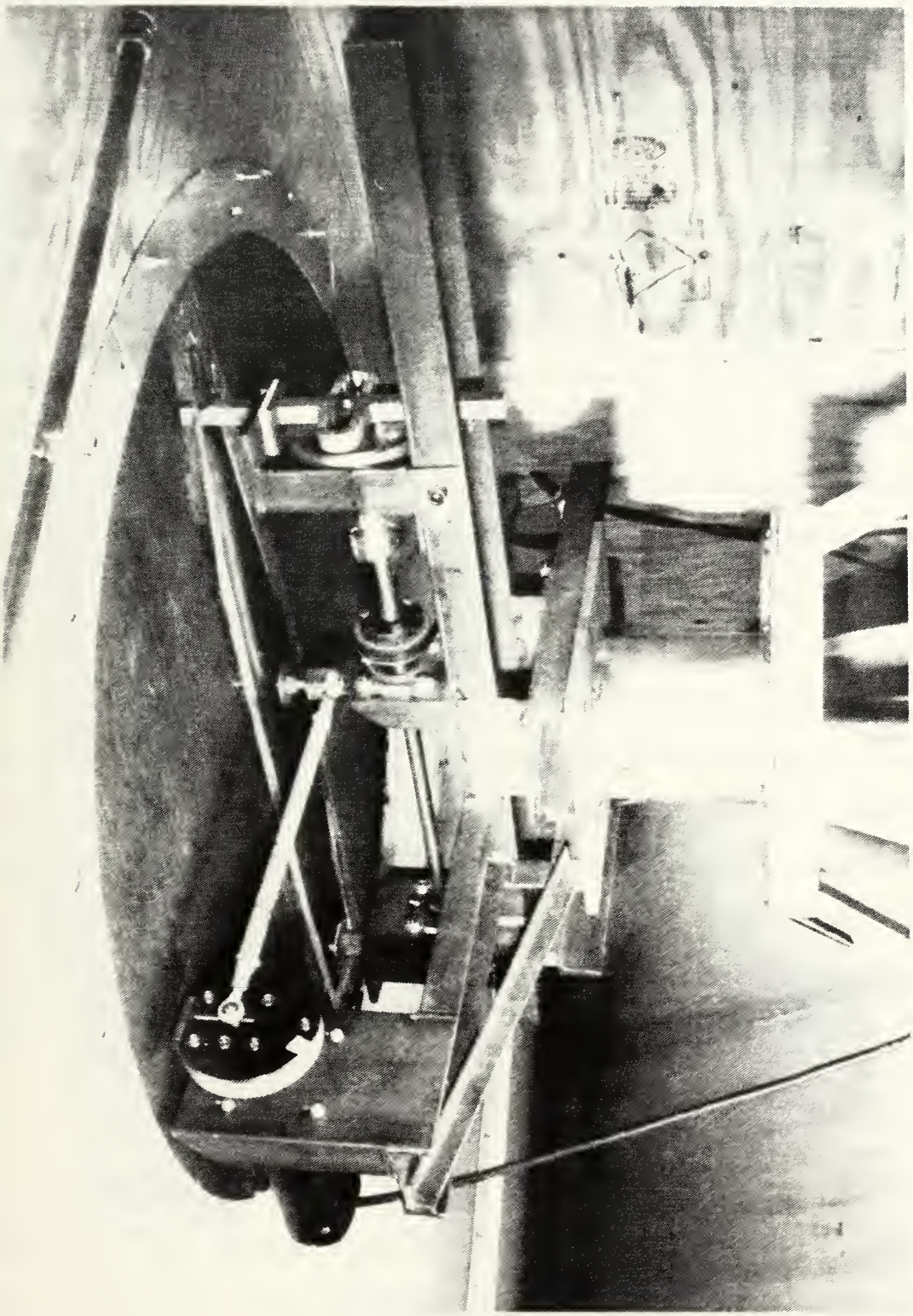

Figure 2. Ship Model Oscillating Mechanism

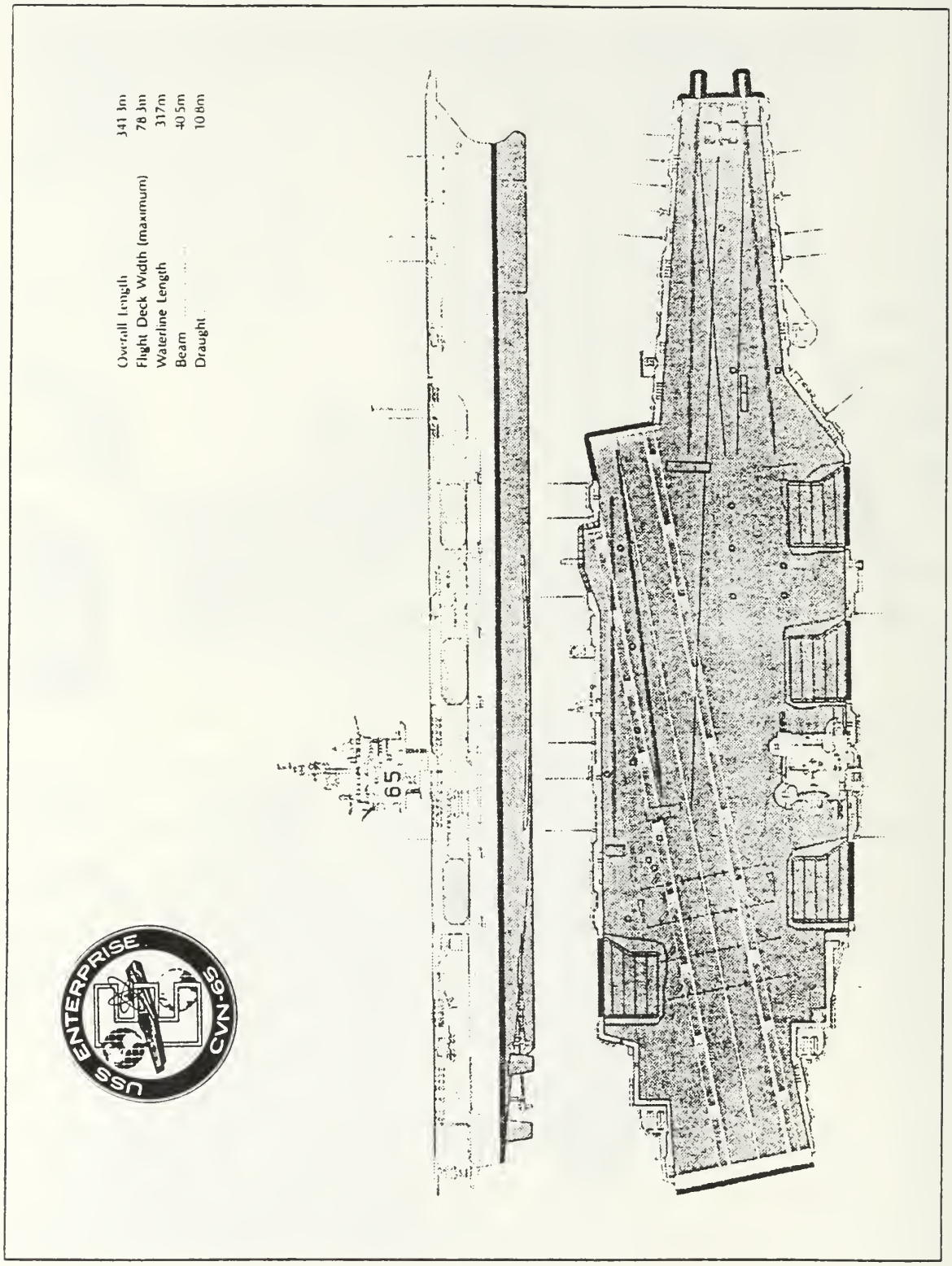

Figure 3. Diagram of the USS Enterprise (CVN-65)

follow-on hot wire anemometry study to extract mean velocity, turbulence intensity and spectrum function information because of its size, the model is believed to be adequate for flow visualization.

Prior to assembly, the hulls of the models were extensively modified internally to accept mounting hardware compatible with the oscillating mechanism, while being mindful of the need for the water line to be even with the floor of the test section. Additionally, the models were spray painted with wrought iron flat black enamel paint to reduce light reflection. The hull, below the water line, was treated with car wax to reduce friction as it rubs against the turntable weather stripping.

Each model was partially assembled according to instructions; the flight deck and superstructure were attached to the hull with a bead of silicon rubber adhesive after the turntable was in place and the hull was mounted to the oscillating mechanism. The three eccentric pins were offset from their flange centers as follows to obtain 1.25° pitch and 6° roll:

* Bow flange: 0.30 inches
* Stern flange: 0.15 inches
* Roll flange: 0.35 inches

The difference in settings between the bow and stern flanges was intentional to account for the center of gravity location (55% of the distance between the bow and the stern)

and to insure that the stern of the model did not break contact with the weather stripping.

The final preparation involved setting the electric motor controls to the correct position to obtain the desired pitch and roll oscillating frequencies. Recall from Table 3 that the model oscillating frequencies desired were 1.74 Hz (105 RPM) and 4.18 Hz (250 RPM) for roll and pitch respectively. Setting the roll motor control knob to 80% of full power consistently achieved the desired roll frequency. The pitch motor, on the other hand, is limited to 3.5 Hz (210 RPM). If the Strouhal number relationship is recalculated to solve for the full scale wind speed, U = 37 knots results, slightly higher that the 31 knots predicated by the atmospheric boundary layer simulation. When employed in this investigation, the pitch motor was operated at 100% power.

Two aircraft carrier models were procured, modified and assembled because of the incompatibility of the two flow visualization techniques utilized in this investigation and discussed in the next chapter.

III. FLOW VISUALIZATION TECHNIQUES

With the model installed in the wind tunnel, interest now turns to making the flow patterns visible. Flow visualization helps one to gain insight into the nature of complex flow phenomena. Flow visualization studies are the starting point for later hot wire anemometry data collection from which can be extracted the information to provide a data bank for simulation studies or guidance for conducting flight operations under adverse conditions. Two techniques that have been employed in the past with varying degrees of success in the flow visualization tunnel, are reviewed with emphasis placed on their application to this investigation.

A. OFF-BODY FLOW TECHNIQUE

1. Helium Bubble System

The helium bubble method of flow visualization is well suited for the study of bluff body air wakes. Neutrally buoyant bubbles closely follow flow streamlines, are durable and can withstand shear forces, and rarely collide with objects in the air stream.

To generate the bubbles, a bubble generating system is employed, manufactured by Sage Action, Inc. of Ithaca, NY. The system, depicted in Figure 4, consists of a console, a high speed head, a vortex filter and clear plastic, flexible tubing that connects the components.

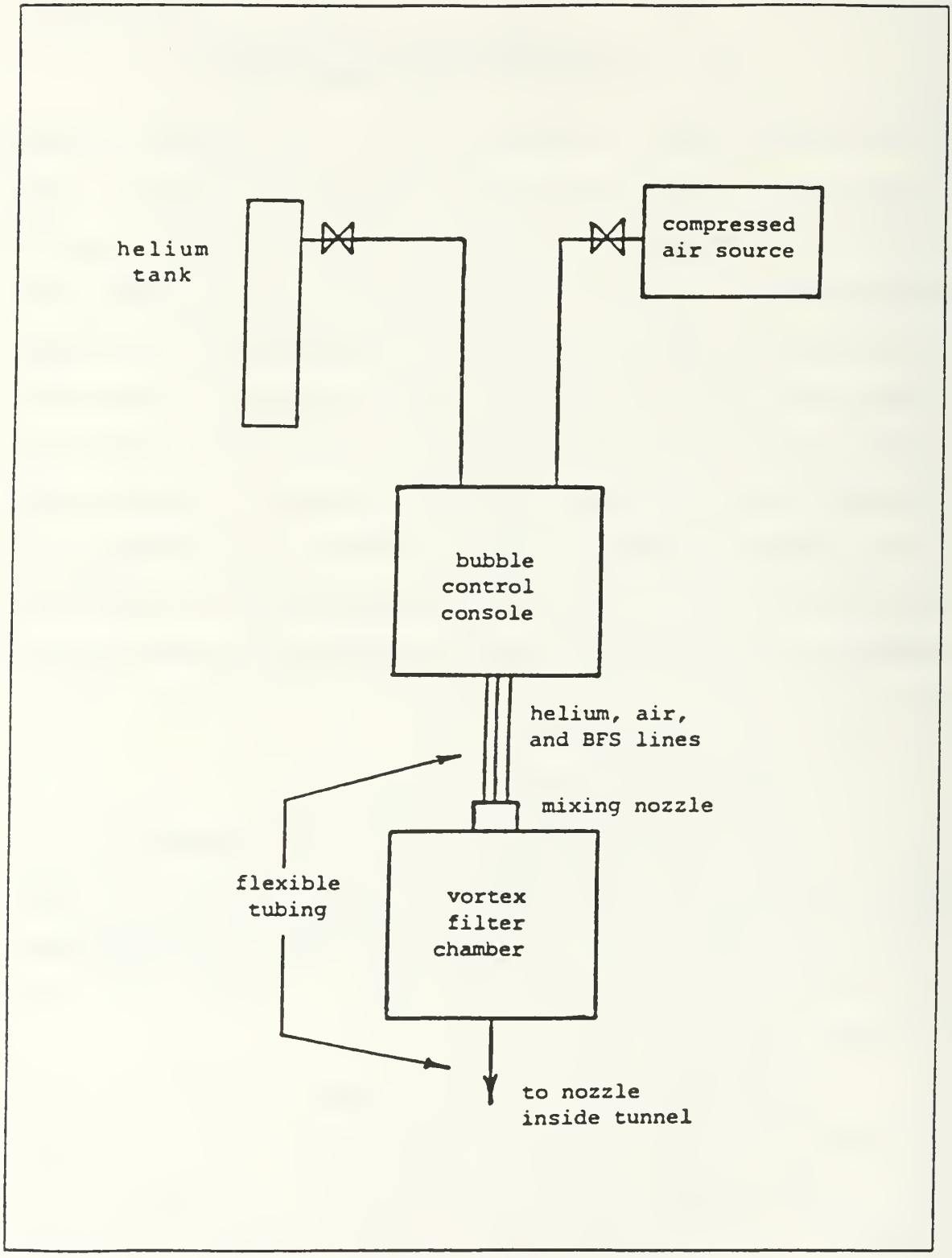

Figure 4. Diagram of the Helium Bubble System
[Ref. 10:p. 29]

Helium from a storage cylinder and compressed air ($\leq$ 50 psi) from a compressor located underneath the tunnel are fed to the console through hose lines. Inside the console is a stainless steel Bubble Film Solution (BFS) storage cylinder with about a five ounce capacity, which is pressurized by the incoming helium. Overfilling the cylinder almost always results in BFS clogging of the helium tubing, and should be avoided. Three on/off toggle switches and micrometering valves control the flow of air, helium and BFS through individual tubing to the high speed head. The toggle switches should be turned on in the proper order (air, helium and BFS) and turned off in reverse order. The micrometering valve positions that consistently provide the maximum bubble generation rate are as follows:

* Air: Full open.
* Helium: 1/4 to 1/2 turn open.
* BFS: 1/2 to 1 turn open.

These three elements come together at the high speed head, which is an arrangement of three concentric tubes. Helium passes through the central needle, BFS through the intermediate tube, thereby forming a bubble with a diameter of about 1 mm at the tip. Air passing through the outer shroud blows the bubble off the tip. The head should be cleaned in warm water after each use to prevent clogging of the small diameter tubes.

The head is mounted to the vortex filter, the function of which is to improve the flow tracing accuracy of the bubbles by allowing only neutrally buoyant bubbles to leave the filter. The bubble carrying jet that leaves the head drives a swirling flow in a clear, plexiglass cylinder. Heavy bubbles (too much BFS) impact the wall of the cylinder while light bubbles spiral inward and burst on the outlet tube. BFS pools at the bottom of the cylinder and can be reused so long as it is poured into a clean container and is set aside to allow the foam to settle. Nearly neutrally buoyant bubbles remain and exit the filter, travel approximately six feet of a 3/8 inch clear flexible tube and enter the tunnel upstream of the model through a simple nozzle mounted on the floor, just downwind of the turbulence generators. This nozzle can be repositioned along the width of the test section to optimize model coverage.

2. Lighting and Photography

Obtaining optimum lighting conditions with the helium bubble technique and achieving subsequent success in capturing on film subtle, as well as significant, flow phenomena, is a time consuming process. Sage Action literature, cited extensively by Mueller [Ref. 14:pp. 343-345], reports that only about 5% of the incident light is reflected by the bubbles. The intensity and placement of the lighting sources, particularly when photographing a large, three dimensional bluff body such as an aircraft

carrier model, directly impact on the quality of the resulting prints. The acquisition of several narrow beam arc lamps is planned in the future. For this investigation, one EIMAC model R-150-5 arc lamp, three 500 watt Sawyers "Rotodisc" slide projectors and one Kodak Ectographic model AF-2 slide projector were placed inside the tunnel, downstream of the test section. Three Kodak AF-2 projectors were placed outside of the tunnel, across from the observation window, in a position to illuminate the model through a small plexiglass window (see the tunnel plan view, Figure 1).

The arc lamp provided the highest intensity light and was consistently employed to illuminate the flight deck. Attempts to utilize the light to illuminate the port side of the model so as to catch shear flow coming up and over the flight deck edge, proved to be fruitless. Although the arc lamp's optical shroud has an adjustable iris diaphragm, a narrow enough beam to illuminate the area without striking the tunnel floor, the hull or the flight deck overhang, was unobtainable.

All of the projectors possessed bright, but wide beams. The method employed to reduce the excess illumination provided by the projectors was to place slide mounting frames, covered with aluminum tape and cut to form narrow slots, in the projectors. The projectors and arc lamp were positioned and elevated or lowered through the use

of wooden blocks, so as to cast light on the bubbles while keeping the ship and floor of the tunnel in the dark. Additionally, self-adhering flock paper was spread all over the tunnel floor to inhibit glare. The use of an overhead lamp, mirrors mounted on the wall and floor, and a bank of fluorescent lamps just below the observation window to provide additional illumination for faint background lighting, proved to be of no help. After considerable trial and error, it was determined that the larger, flat area dimensions of the aircraft carrier model and its reduced superstructure development, as compared to the generic destroyer model employed by Bolinger [Ref. 8] and Biskaduros [Ref. 10], required that the lighting be placed approximately an inch above and just to the side of the model to reduce glare. This measure insured that no part of the model would be illuminated when undergoing oscillation. The projectors frequently had to be adjusted because of their tendency to move due to fan motor induced vibrations in the tunnel.

The camera utilized for this study was the Hasselblad 2000 FCW single lens reflex camera. A Zeiss 150 mm, f2.8 wide aperture lens was exclusively used to shoot all photographs. A protective haze filter and a lens hood were installed. Lack of a light meter or automatic exposure feature in the camera is compensated by the ability to rapidly interchange different film magazines. As a starting

point, the aperture setting and shutter speed combinations that were successful in previous investigations [Refs. 8,10] were set and Polaroid 107C black and white 3000 ASA film was shot. The immediate feedback provided by the Polaroid picture led to adjustment of the camera exposure value or the tunnel lighting. Upon achieving a satisfactory photograph, one that recorded distinct pathlines and appropriate coverage, the Polaroid magazine was exchanged for one containing Kodak TMAX 400 ASA, 120 mm film. To achieve the same results with this professional format, high resolution film, opening the aperture setting approximately one f-stop and requesting that the film be "pushed" to 1600 ASA in the development process, was required. The occurrence of lighting changes due to infrequent fluctuation of bubble flow or during ship motion oscillation, created the need to take at least four and as many as 12 shots of each pose. To increase the likelihood of obtaining a satisfactory TMAX print, the f-stop on either side of the one selected from Polaroid print analysis, were also set and shot. It is interesting to note that of the 24 helium bubble photographs selected for inclusion in this report, six were shot at an aperture setting one half an f-stop more open than that used to take the Polaroid print, 12 were shot with a more open aperture setting of one f-stop and finally, six were shot at a more open aperture setting of one and a half f-stops.

To summarize the procedure: Once the ship model has been posed, adjust the lighting, turn on the tunnel and helium bubble system, and shoot Polaroid pictures. An f8 aperture setting and a shutter speed of one and a half seconds serves as a good starting point. Once a satisfactory print has been obtained, exchange film magazines and open the aperture one and a half stops, shoot TMAX and repeat the process two more times, closing down the aperture by half an f-stop each time. For example, if f8 resulted in a good Polaroid print, then shoot TMAX film at f4/5.6, f5.6 and f5.6/8. The shutter speed does not change.

B. ON-BODY FLOW TECHNIQUE

1. Fluorescent Minitufts

The use of tufts for flow visualization is a well known technique that is advanced to a sophisticated level with the use of extremely thin fluorescent nylon monofilament material. Crowder [Ref. 15] developed the use of fluorescent minitufts, though he recognizes that while large area separation can be revealed, small separation areas are not made visible with this technique [Ref. 15: p. 55]. The idea behind this method is to obtain a qualitative feel for local turbulence intensities. The direction which individual tufts point with respect to the wind gives an indication of the location and level of separation.

By following the technique outlined by Crowder [Ref. 15], as modified by the lessons learned by Bolinger [Ref. 8: pp. 32-34], the time consuming placement of tufts on one of the USS Enterprise (CVN-65) models was undertaken. Tools that were essential to complete the task included a Spectroline Model Q-22FA lamp, UVS-30 spectacles, an assortment of hobby knives, cuticle scissors, tweezers, scotch tape, 1/2 inch flat paint brushes, "super glue" pens and finger nail polish remover (containing acetone). The lamp, a four tube unit with two ultra-violet (UV) tubes on one ballast and one UV and one white light tubes on the other, possessed a magnifier and was mounted on a flexible arm. The lamp was indispensable in handling the minituft material. To counter the effects of prolonged exposure to long wave UV radiation, clear spectacles were utilized, both while tufting the model and while running the wind tunnel experiment. Both the lamp and the spectacles are available from the Spectronics Corporation, Westbury, NY.

After the model was spray painted a flat black color, a grid was laid out that resulted in the creation of evenly spaced 0.5 by 0.25 inch rectangles. Significant features of the model, such as the water line, flight deck edge,and superstructure, were outlined with 0.0019 inch diameter minituft material, so that the general profile of the ship would be visible in the presence of UV light. The minitufts themselves were made from 0.0007 inch diameter

material. About eight inches of this ten-strand yarn was removed from its spool and was taped at both ends. One strand was plucked from the yarn and laid out on the grid. The two ends were secured into place with very small beads of super glue that had been allowed to become tacky through exposure to air for approximately a half hour. This process was repeated until the model surface was covered. With the minituft material laid out, small drops of adhesive were applied at 1/2 inch intervals in conformity with the grid. When the glue dried, one end of the minituft was cut from the glue bead and the 1/2 inch tuft was brushed and blown into a vertical position. The presence of "static cling" was overcome by the frequent application of anti-static spray to the brush that combed the minitufts. The minituft material is manufactured by the X-Aero Company of Bellevue, WA.

2. Lighting and Photography

Two types of UV lighting schemes were employed to obtain interpretable photographs. The first technique employed the two working ballasts of a four tube bank of fluorescent lights mounted below the observation window. "Black light" tubes were in place in the two ballasts (the other two were inoperative). The glass of the tubes contained filter material which is opaque to most visible light but freely transmitted long wave UV light.

Time-elapsed photography utilizing the UV fluorescent tubes was attempted. Based on previous experience of Bolinger [Ref. 8:pp. 33-34], a shutter speed of four seconds was anticipated. The appropriate aperture settings of f5.6 and lower were obtained through trial and error. This lighting scheme was used on non-oscillating model photographs. Note that depth of field becomes a problem when shooting with a wide aperture lens at a low f-stop. Part of the subject will be out of focus; this can only be remedied by increasing the lighting or by moving the camera away from the subject.

The second lighting technique utilized a Norman 2000 flash unit and a UV transmitting filter. The flash unit, manufactured by Norman Enterprises, Inc. of Burbank, CA, has an available output of 400 to 2000 watt-seconds, in 400 watt-second intervals. After considerable trial and error, 2000 watt-seconds was selected for all photographs. The flash unit consisted of a lamp head with a cooling blower, a reflector, a honeycomb grid and a locally manufactured UV transmitting filter. The filter was made from two 6 x 12 inch plates of Corning 5970 UV transmitting, visible absorbing filter glass. The plates were cut into 64, inch and a half squares. The edges of the squares were roughened with a belt sander and the squares were reassembled, with the help of silicon rubber adhesive, into four 3 x 3 inch squares containing 16 of the inch and a half squares each.

Stock aluminum H-channel was manufactured into a cross and the four 3 x 3 inch glass squares were placed in the four quadrants of the cross. Stock aluminum U-channel and mirror mounts were used to frame the filter. This elaborate procedure to make the filter was followed because of the high thermal expansion coefficient of the glass. It was feared that repeated exposure to head lamp flashes might easily crack the filter if it were in larger pieces. The UV filter was mounted to the front of the honeycomb grid with three inch clear tape.

The flash unit itself was mounted to a strap of angle iron installed above the observation window. Employment of the flash unit revealed that visible light leaked out from the reflector; the whole flash unit was subsequently covered with flock paper, but some leakage still existed. For flash photography, the shutter was set to "B" (untimed). After opening the shutter, the flash was manually triggered and the shutter was closed. Oscillating model photographs were taken with this lighting scheme. Aperture settings of f4 resulted in good TMAX prints, although white light leakage slightly washed out the prints.

The camera used for all of the UV photography was the Hasselblad 2000FCW previously discussed. Needed, however, was the ability to filter out reflected UV light while allowing the fluorescence of the tufts to reach the film. A Kodak Wratten gelatin filter was available for use

but after consultation with photographic equipment specialists, it was determined that no known means of mounting the filter to the Hasselblad "F" type lens was available. The solution to this problem was to cut a 2.4 inch diameter circle out from the center of the 150 mm lens cap. A rigid Kodak 75 mm^2 gelatin filter holder was then mounted to the lens cap with silicon rubber adhesive. The modification worked well. The NPS Aeronautical Engineering Department has recently acquired a Nikon N2000 35 mm single lens camera which has many popular features, except auto-focusing. The department also has a Kenko filter holder and a 62 mm to 52 mm step up ring, suitable for mounting the Wratten filter. Since TMAX 400 is also available in the 35 mm format, future UV photography should be attempted with the Nikon camera.

IV. RESULTS AND DISCUSSION

A. SCOPE OF THE INVESTIGATION

The level of model detail, its size and the range of motion available, require that bounds be put on this study. It was decided that for this report, the principal flight operation axes of the aircraft carrier would be studied in detail. Both for fixed wing and rotary wing aircraft, winds down the bow (0^{o} yaw) and down the angled deck (12^{o} port yaw) are the heart of the launch and recovery envelope.

In order to determine the sensitivity of the model's response to slight changes to its profile presented to the free stream wind, the full range of motion available from the model oscillating mechanism was exercised. For the two yaw angles selected, the following six poses were photographed:

1. 0^{o} pitch, 0^{o} roll
2. 1.25^{o} up pitch, 0^{o} roll
3. 1.25^{o} down pitch, 0^{o} roll
4. 0^{o} pitch, 6^{o} port roll
5. 0^{o} pitch, 6^{o} starboard roll
6. Oscillating pitch and roll

As previously discussed, a 150 mm telephoto lens was used for all of the photographs to capture as much detail as possible. A drawback of using this lens was that the model

had to be shot twice in order to properly cover the bow and stern of the ship. The poses were repeated and photographed for the two different flow visualization techniques, as well. The resulting number of photographs contained in this report is 48.

Before proceeding to the photographs, a description of the flight deck environment and the topics of concern to rotary and fixed wing operations, is appropriate. Figure 5 is a diagram of the typical aircraft carrier flight deck, USS Kitty Hawk (CV-63) class or later. Five helicopter spots are defined, two on the bow and three on the angled deck. With an air wing embarked, day/VFR helicopter operations are normally run from spot 3, while at night, operations are conducted from spot 4 so as to provide the visual cue of a airborne run down the angled deck to the pilot prior to entering total darkness. The location of the spots is a compromise between the need to have maneuvering room on deck to re-spot aircraft and the need to minimize the amount of rotor blade diameter that is subject to shear flow coming up and over the deck edge. The hazards to helicopters resulting from shear flow include the possibility of a blade folding up in the vertical or, in the case of a tandem rotor helicopter (CH-46), the unintentional striking of the synchronizing shaft tunnel.

Fixed wing aircraft are launched from four catapults, two located on the bow and two located on the angled deck.

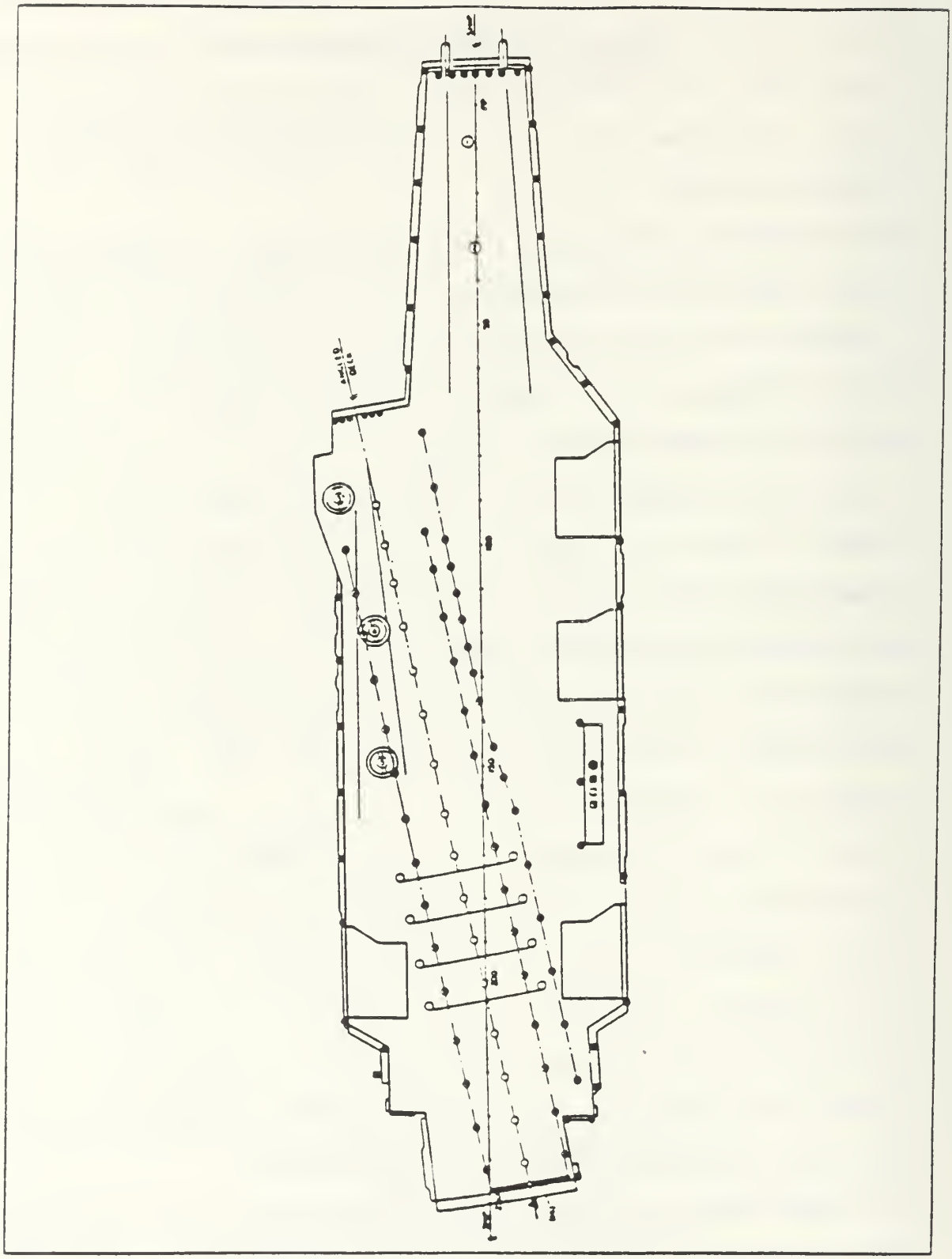

Figure 5. Diagram of CV Flight Deck

The optimum recovery wind speed down the angled deck is between 25 and 30 knots. The air wake created by the superstructure, coupled with the angle and magnitude of any cross wind determine the level of turbulence an aircraft flies through to touch down. The "burble" is a much discussed phenomena that is attributed to starboard winds that drive the turbulent superstructure air wake into the landing area, thereby causing a sudden reduction in the free stream velocity reaching the approaching aircraft. Increased aircraft sink rate and possible damage result if not compensated by pilot action.

These topics are worthy of research. It is hoped that this paper serves as a benchmark for the comparison of results.

B. ZERO DEGREE YAW

In general, the flow over the bow of the model is very smooth. Some bubble traces on the port side sweep up and over the flight deck edge and merge with the other pathlines. This activity becomes more pronounced when the bow is raised (Figure 8a). Note also that the oncoming free stream flow striking the bow climbs over the edge, then conforms to the general direction of the pathlines. Further work needs to be done to determine if and when re-attachment occurs. This phenomenon is not as pronounced when the bow is lowered (Figure 10a). There is no noticeable change in the superstructure air wakes recorded in Figures 7a, 9a and

11a. However, when the model is rolled, a distinct phenomenon is observed. A port roll (Figure 13a) appears to accentuate the separation, creating a relatively long stream of eddies in the superstructure air wake. A starboard roll (Figure 15a) appears to diminish the turbulence in the air wake; while separation occurs, the vortices generated behind the superstructure are less intense. The initial reaction to this observation is to attribute it to poor lighting. Detail is lost in Figure 15a because the side lighting has to be raised to reduce glare coming off the flight deck. Nonetheless, if one compares the bubble traces at the "round down," the rear edge of the flight deck where the lighting is not compromised, one notices that significant turbulence still exists in the flow when the model is in a port roll (Figure 13a) as opposed to when it is in a starboard roll (Figure 15a). When the model oscillates (Figures 16a and 17a), the flow on the bow (Figure 16a) is not significantly different from the flow fields observed earlier. The superstructure air wake is significantly more turbulent, an observation that can be attributed to ship motion forcing the flow field. Recall that the pitch oscillating frequency is 3.5 Hz and the roll frequency is 1.74 Hz. In order to obtain bubble traces with the available light and without resorting to a low f-stop that would affect the depth of field, a two second shutter speed was selected. During that exposure time, the ship experienced seven pitch and three

and a half roll cycles. The ability to capture approximately one cycle on film, which might be of more analytical value, is not possible with the current lighting available.

The fluorescent minituft photographs serve to confirm the general smoothness of the flow on the flight deck. All of the photographs taken were time-elapsed shots, except for those involving oscillation (Figures 16b and 17b). The minitufts on the flight deck, including those on the deck edge, conform to the direction of the free stream flow. For the time-elapsed photographs, the minitufts on the hull (bow, port side) are blurred, an indication of very turbulent flow. The only significant activity detected is around the superstructure where the minitufts bend and follow the circulation and reverse flow present in the air wake. The minitufts in place behind the superstructure, point in the general direction of the flow, well before the round down, an indication that the reversed flow region ends well upwind of the stern.

C. TWELVE DEGREE STARBOARD YAW

Separation of the flow is immediately observed on the bow as the model is yawed. The phenomenon appears to be enhanced when the bow is raised (Figure 20a) or when the model is rolled to starboard (Figure 26a), occasions when a greater surface area is presented to the oncoming free stream flow. Immediately, one thinks of helicopter spots 1

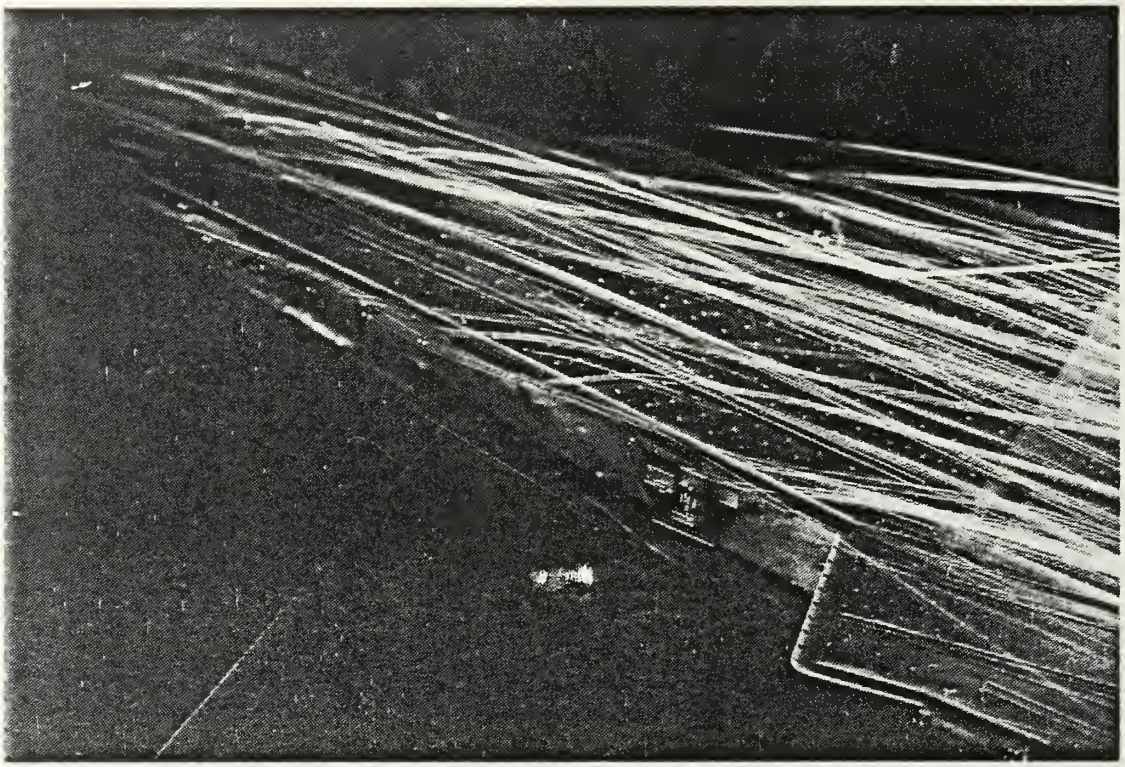

(a) Helium Bubble

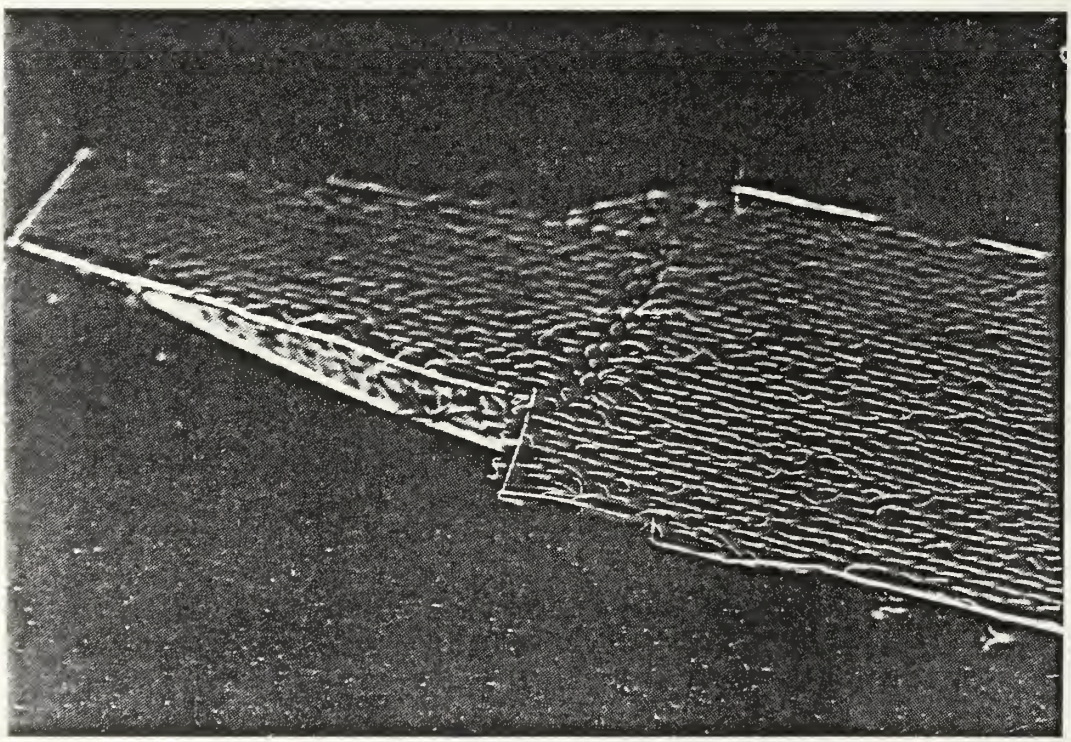

(b) Fluorescent Minituft

Figure 6. Forward: 0^{o} Yaw, 0^{o} Pitch, 0^{o} Roll

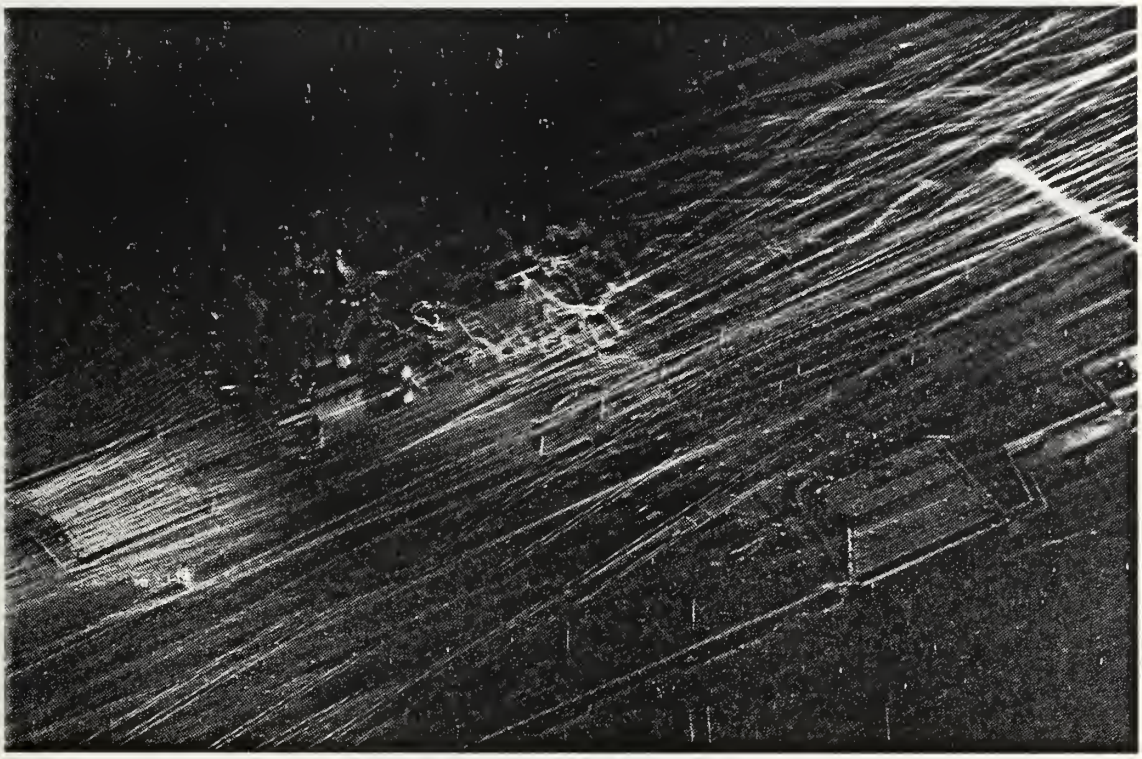

(a) Helium Bubble

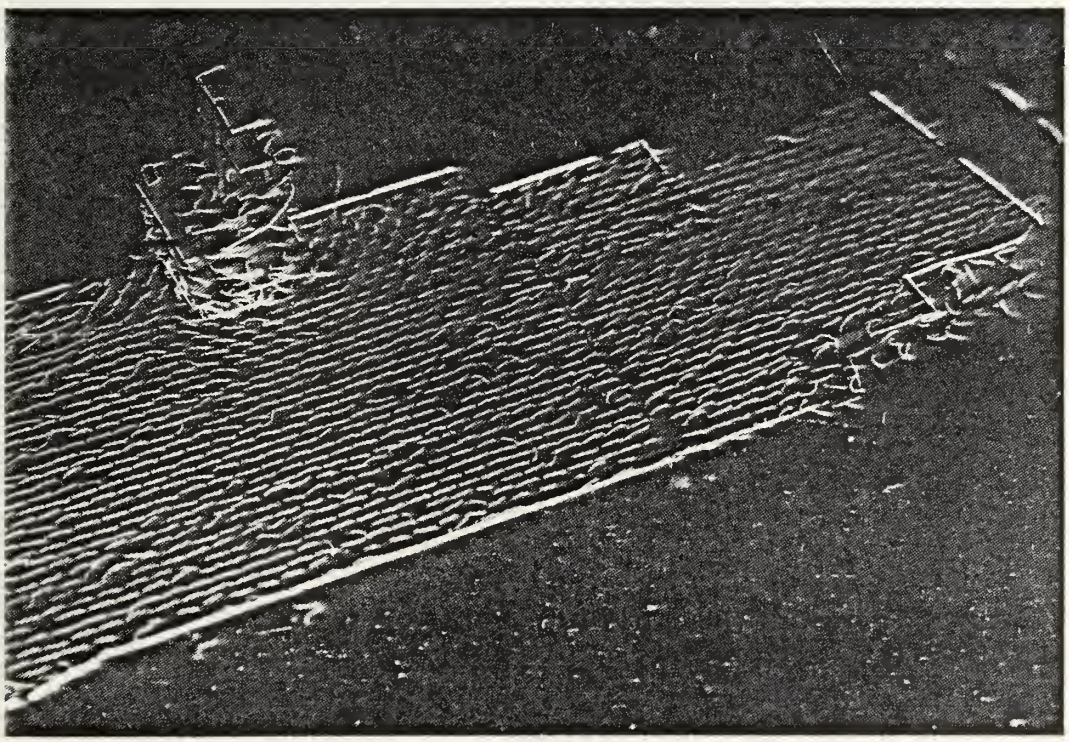

(b) Fluorescent Minituft

Figure 7. Aft: 0^{o} Yaw, 0^{o} Pitch, 0^{o} Roll

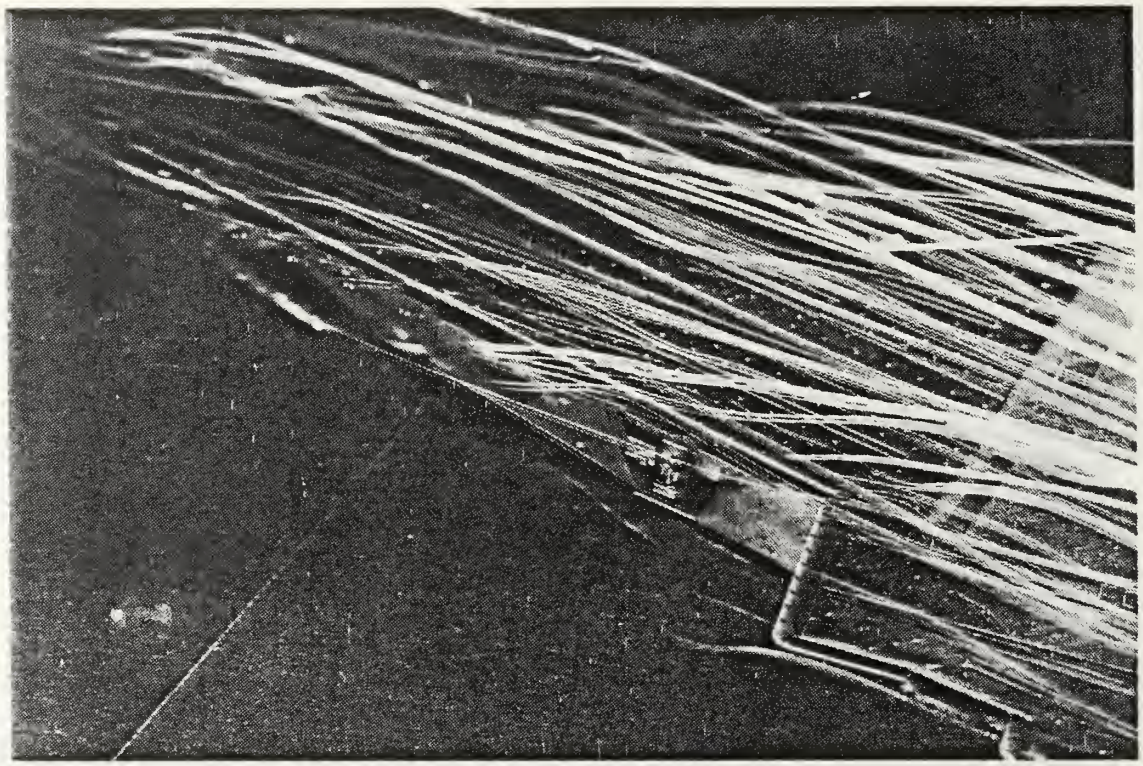

(a) Helium bubble

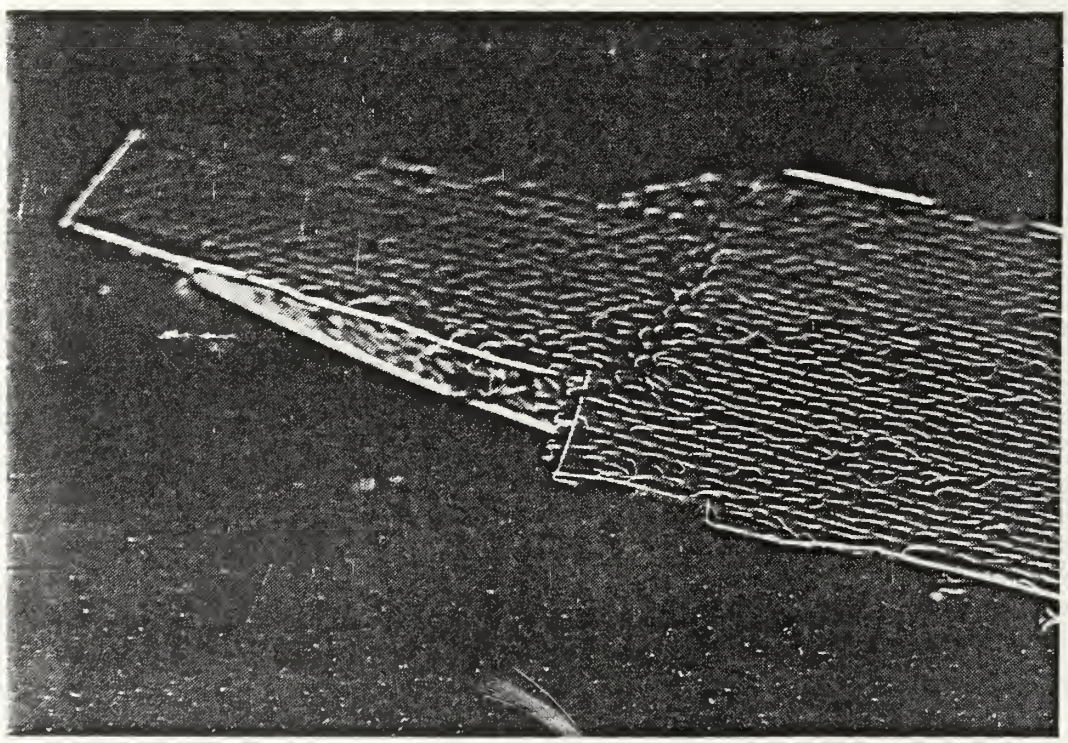

(b) Fluorescent Minituft

Figure 8. Forward: 0^{o} Yaw, 1.25^{o} Up Pitch, 0^{o} Roll

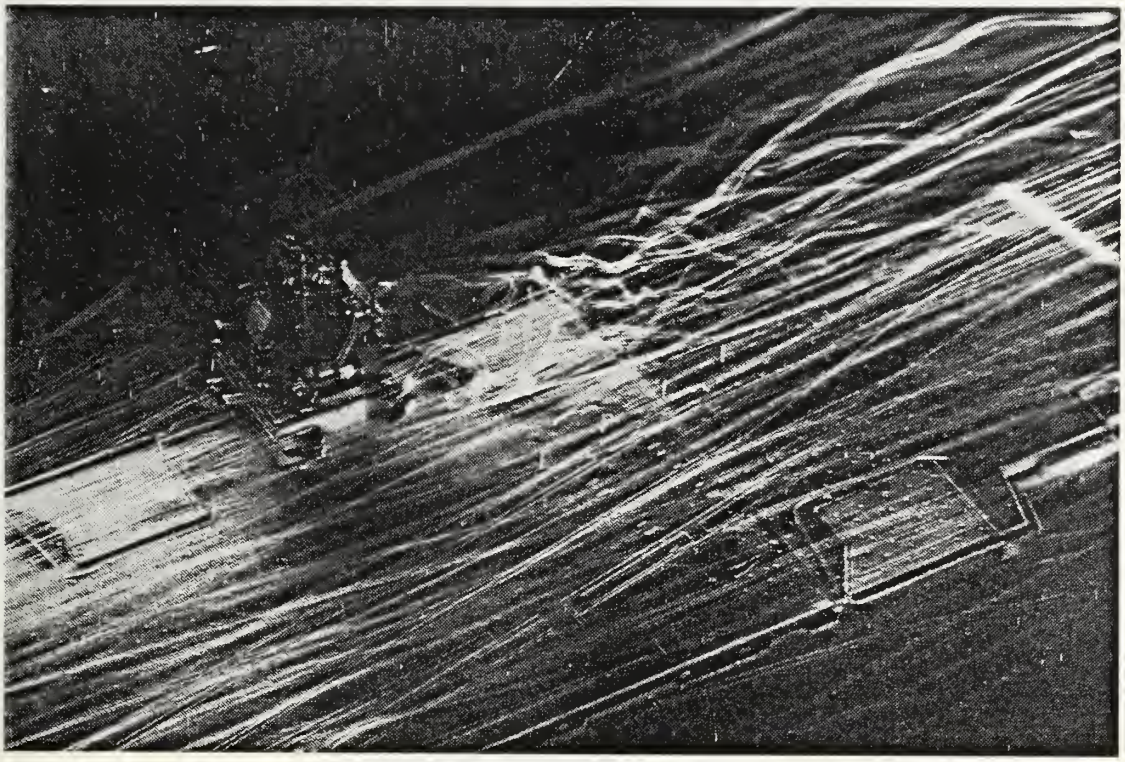

(a) Helium Bubble

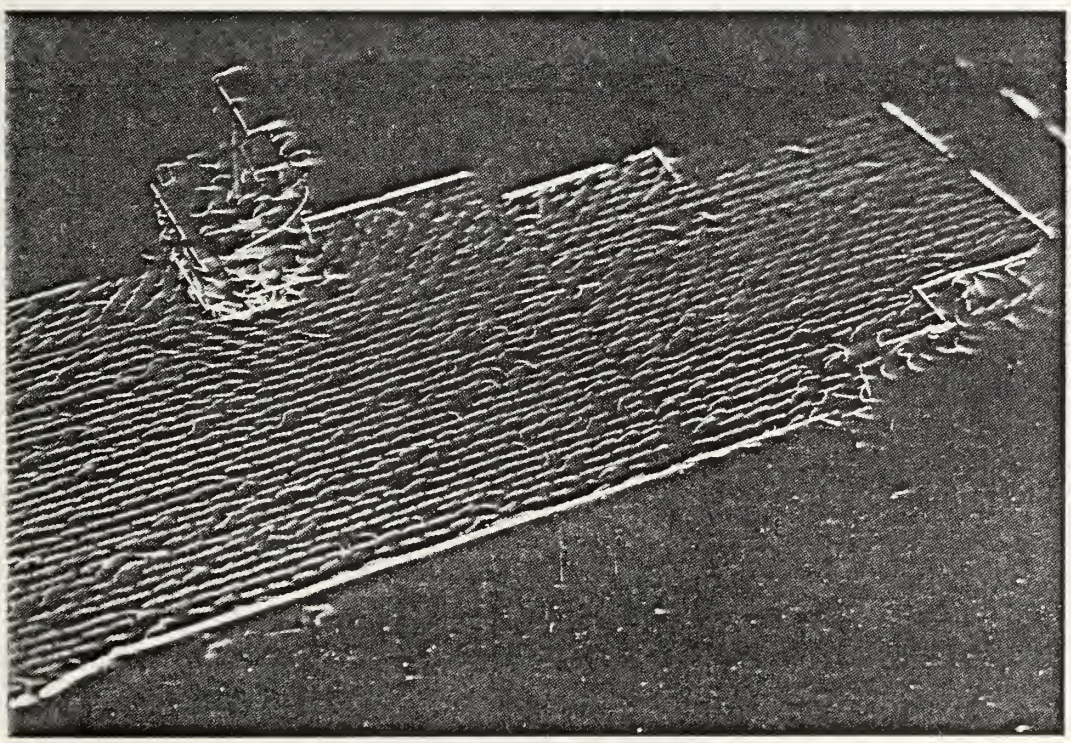

(b) Fluorescent Minituft

Figure 9. Aft: 0^{o} Yaw, 1.25^{o} Up Pitch, 0^{o} Roll

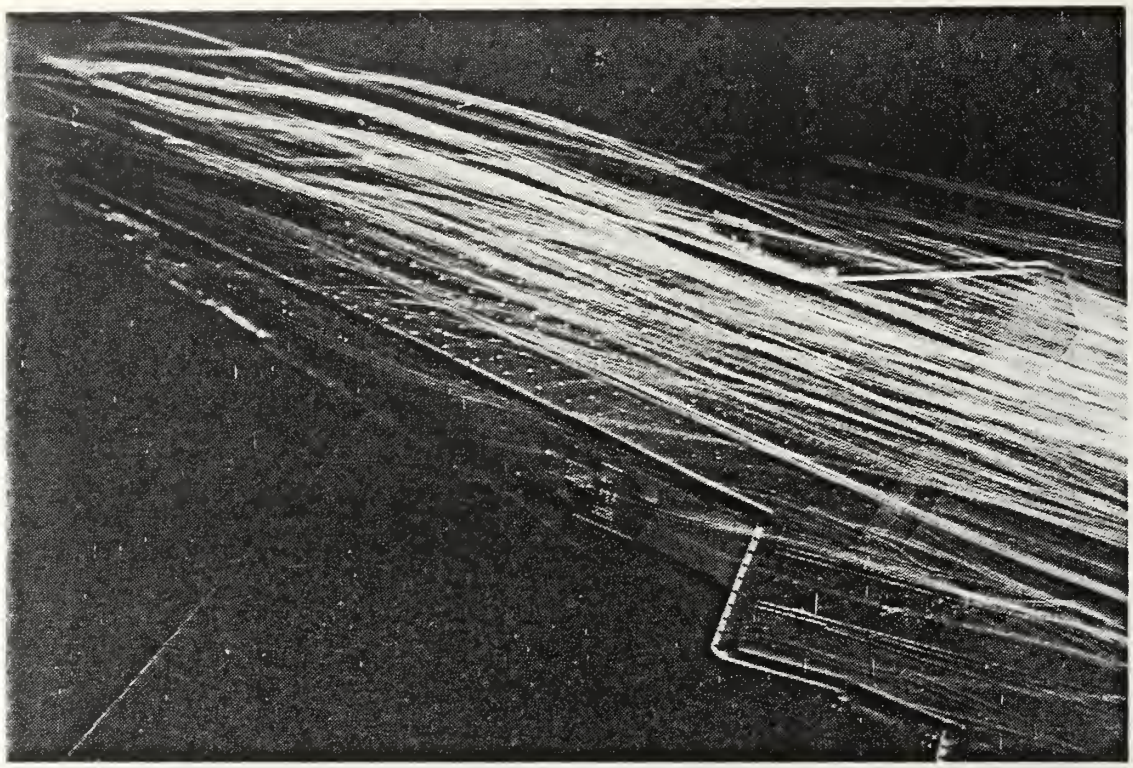

(a) Helium Bubble

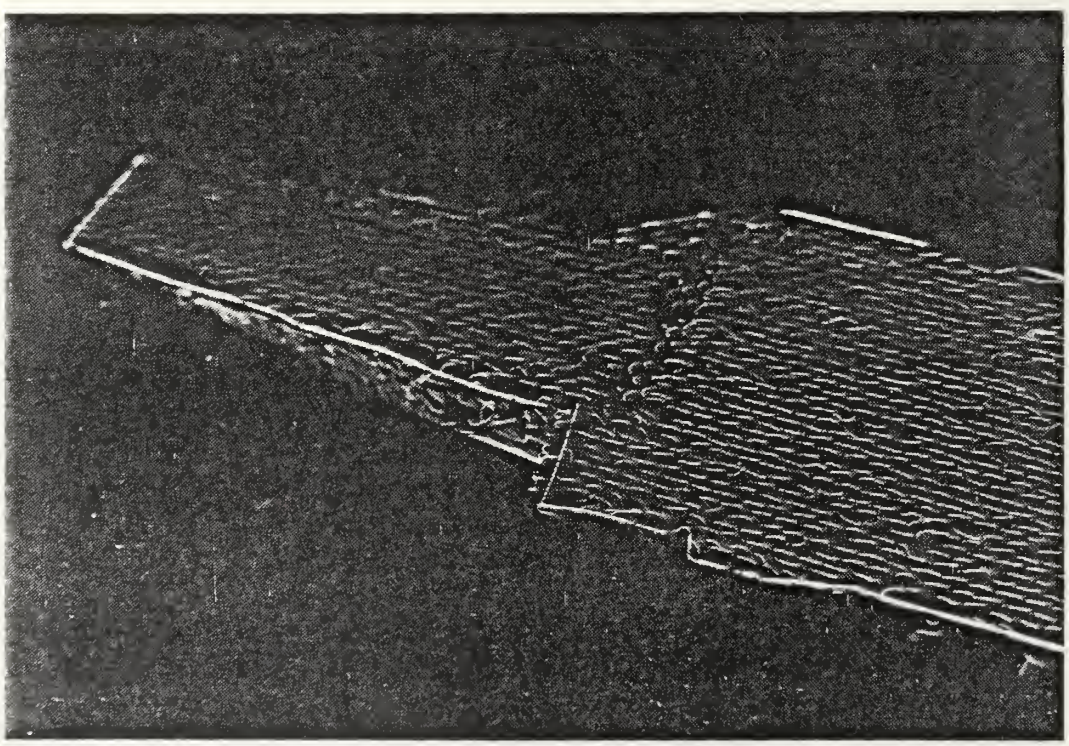

(b) Fluorescent Minituft

Figure 10. Forward: 0° Yaw, 1.25° Down Pitch, 0° Roll

(a) Helium Bubble

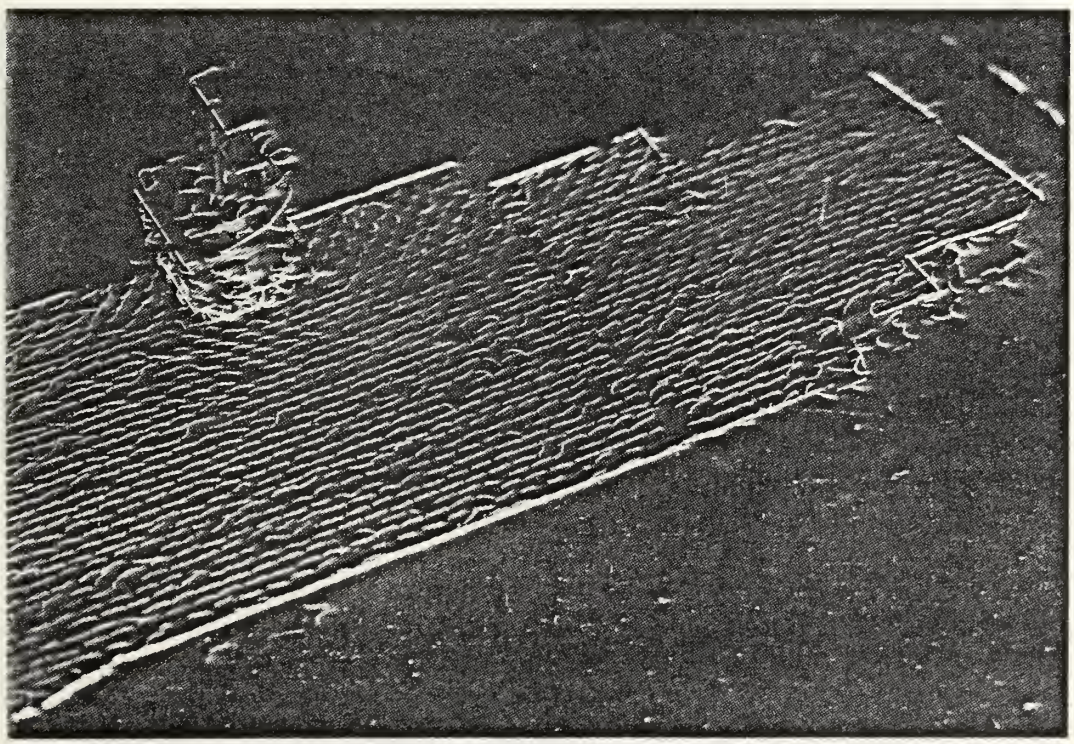

(b) Fluorescent Minituft

Figure 11. Aft: 0^{o} Yaw, 1.25^{o} Down Pitch, 0^{o} Roll

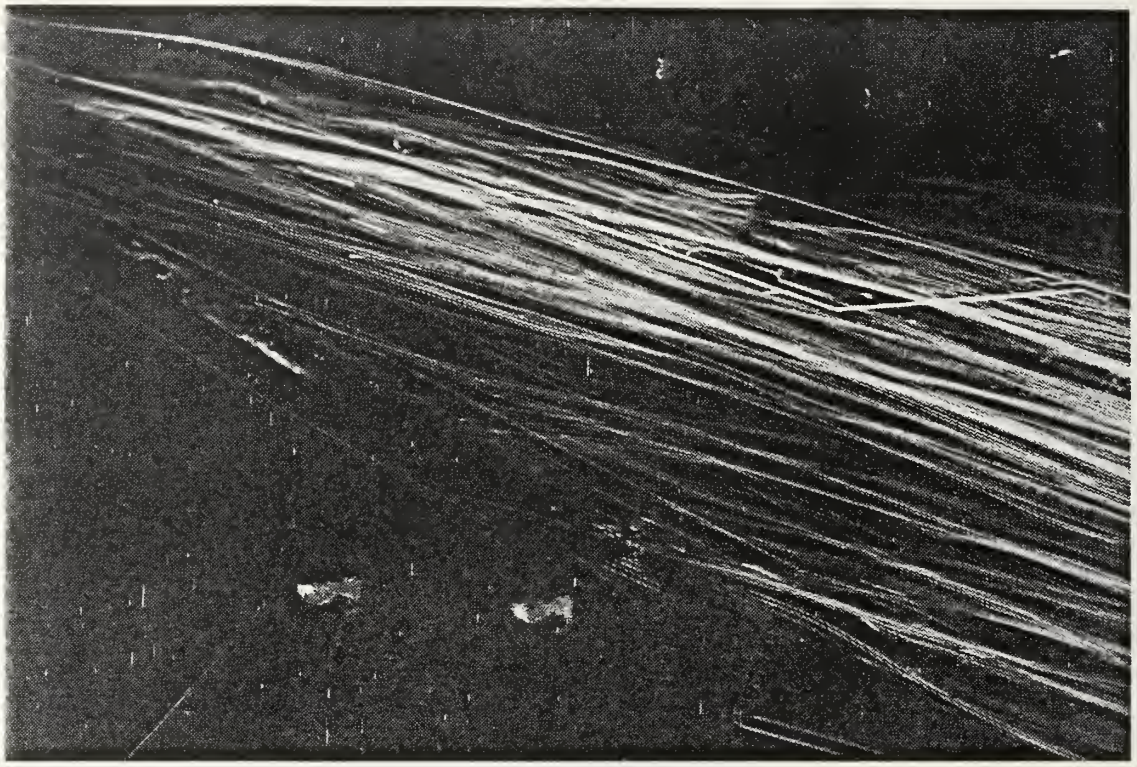

(a) Helium Bubble

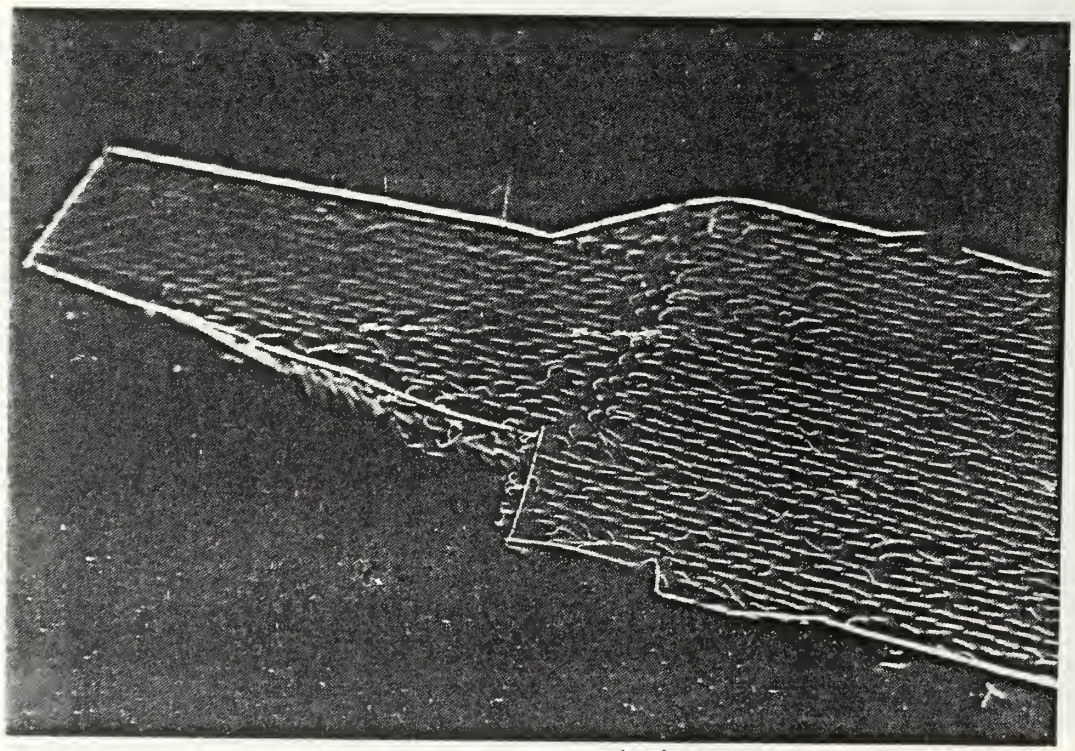

(b) Fluorescent Minituft

Figure 12. Forward: 0^{o} Yaw, 0^{o} Pitch, 6^{o} Port Roll

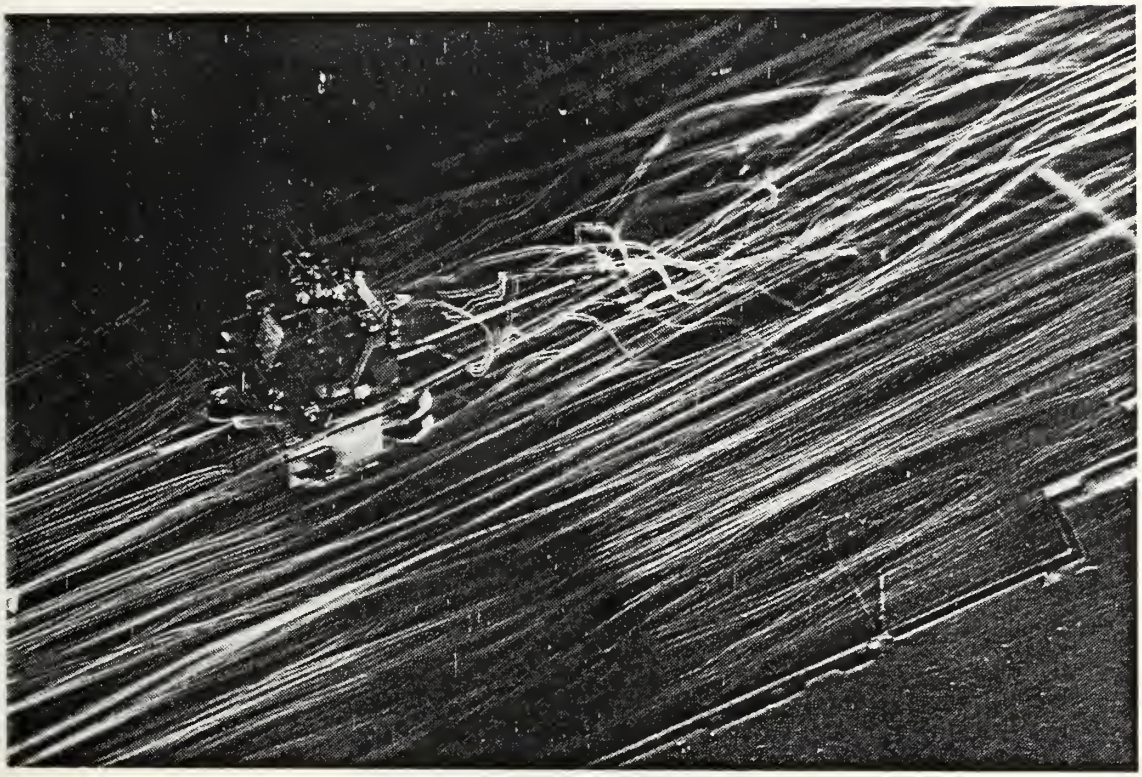

(a) Helium Bubble

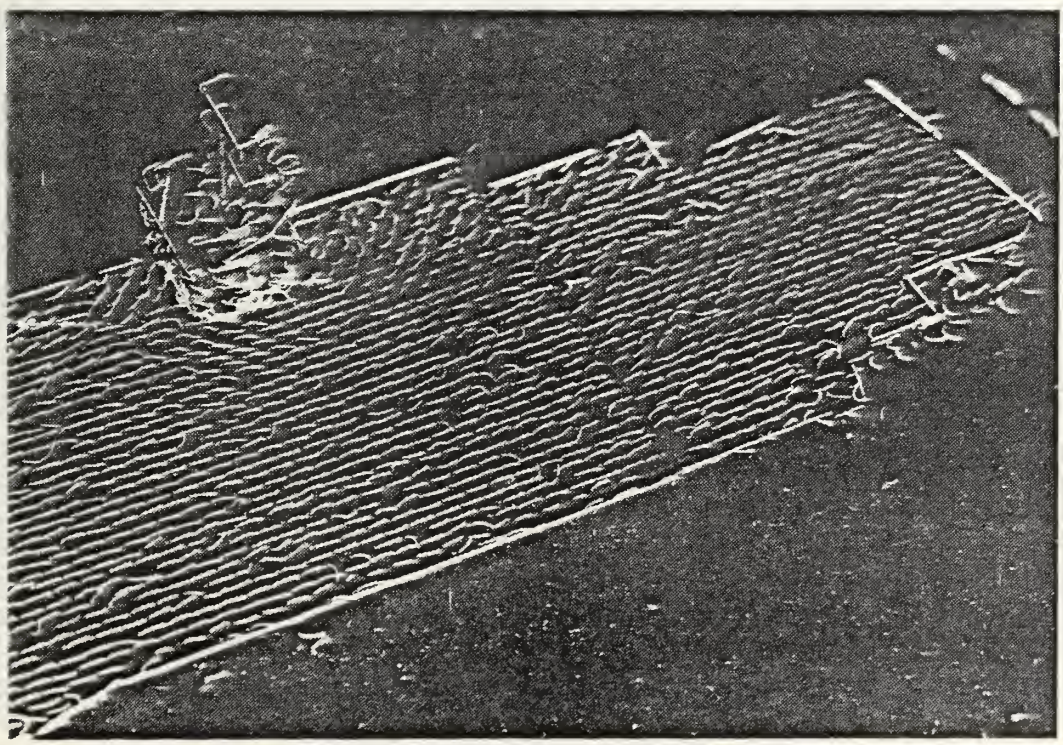

(b) Fluorescent Minituft

Figure 13. Aft: 0^{o} Yaw, 0^{o} Pitch, 6^{o} Port Roll

(a) Helium Bubble

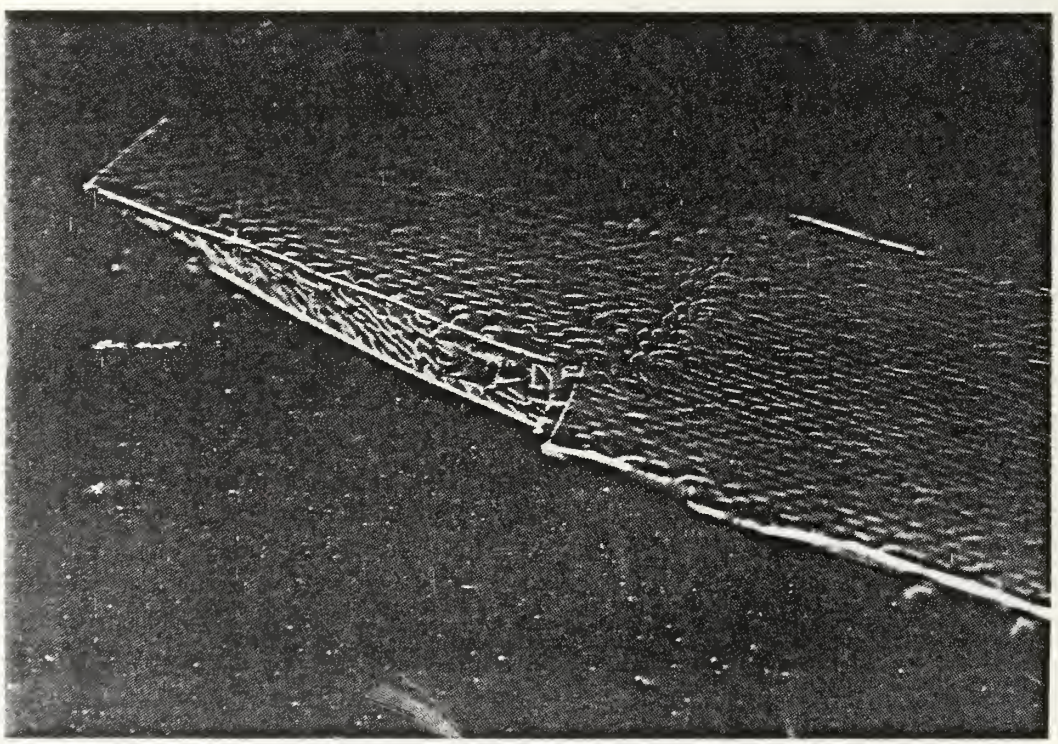

(b) Fluorescent Minituft

Figure 14. Forward: 0^{o} Yaw, 0^{o} Pitch, 6^{o} Starboard Roll

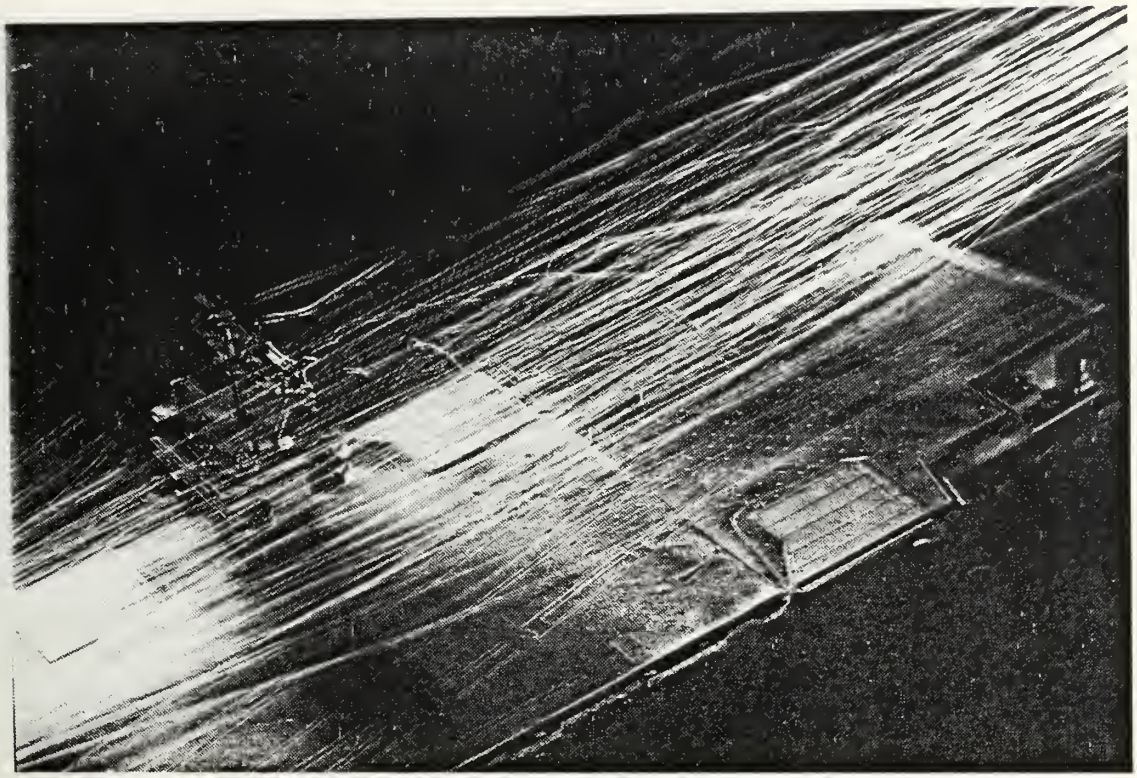

(a) Helium Bubble

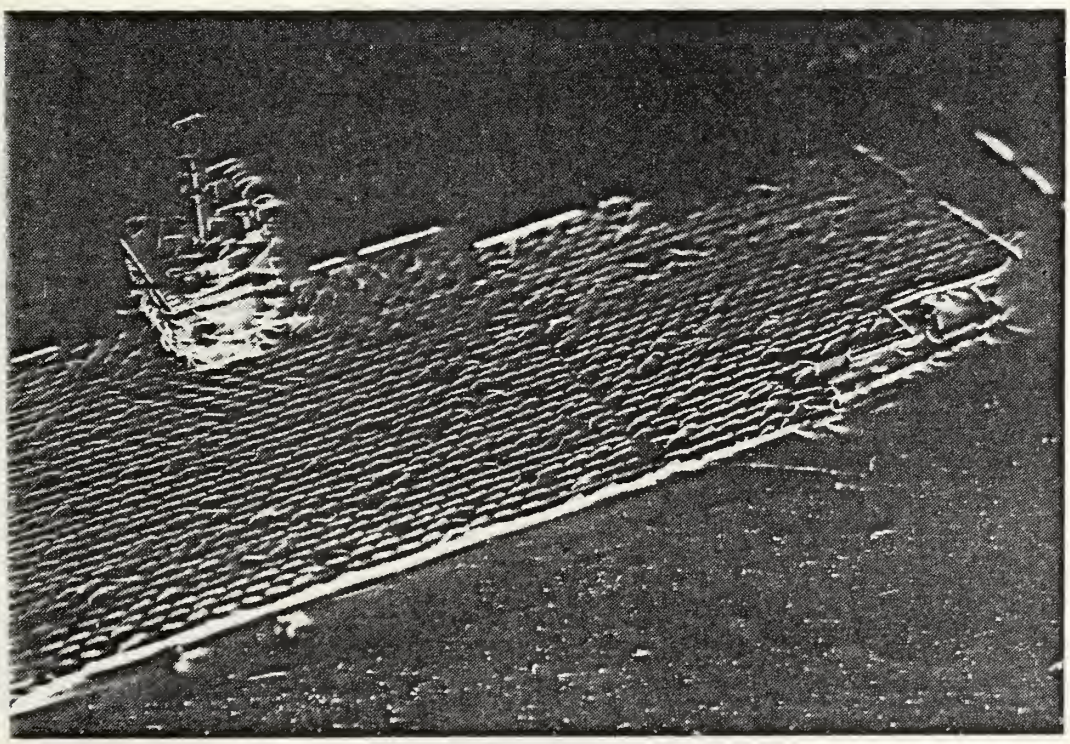

(b) Fluorescent Minituft

Figure 15. Aft: 0^{o} Yaw, 0^{o} Pitch, 6^{o} Starboard Roll

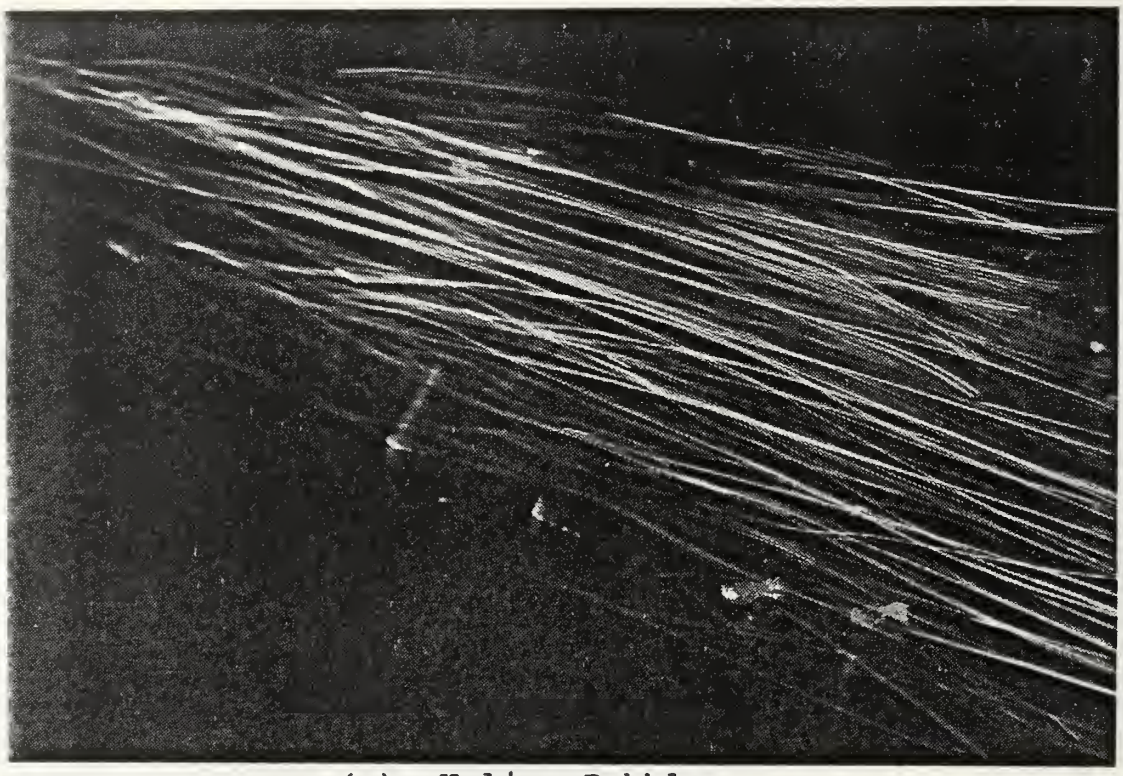

(a) Helium Bubble

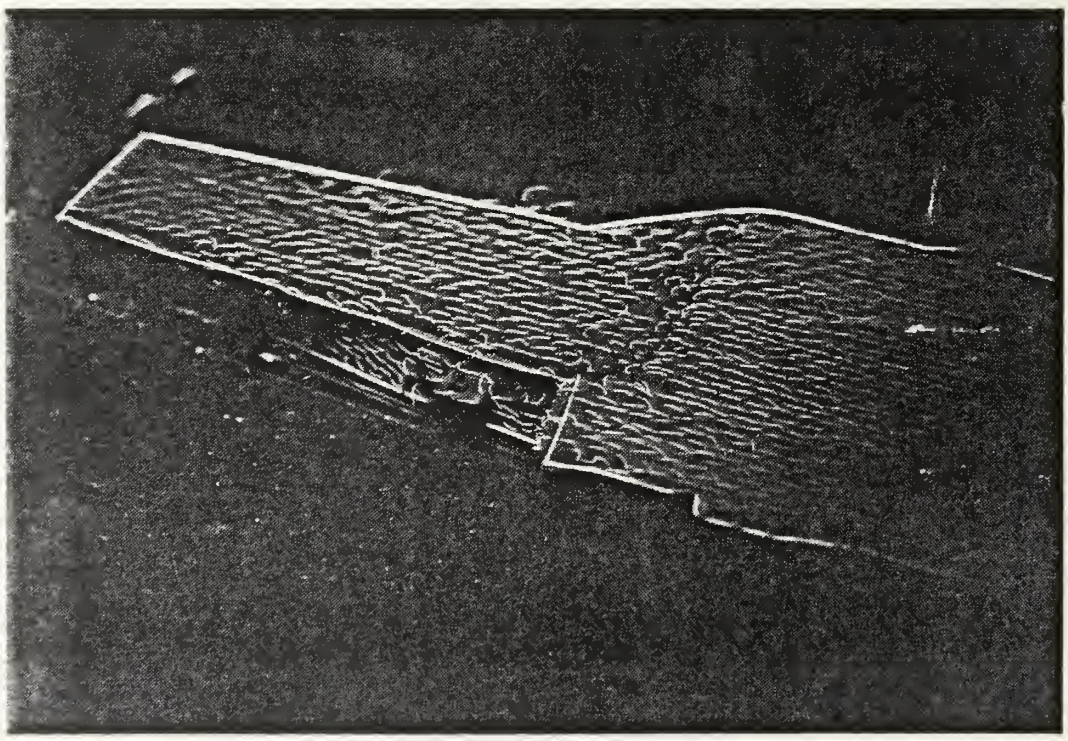

(b) Fluorescent Minituft

Figure 16. Forward: 0^{o} Yaw, Oscillating Pitch and Roll

(a) Helium Bubble

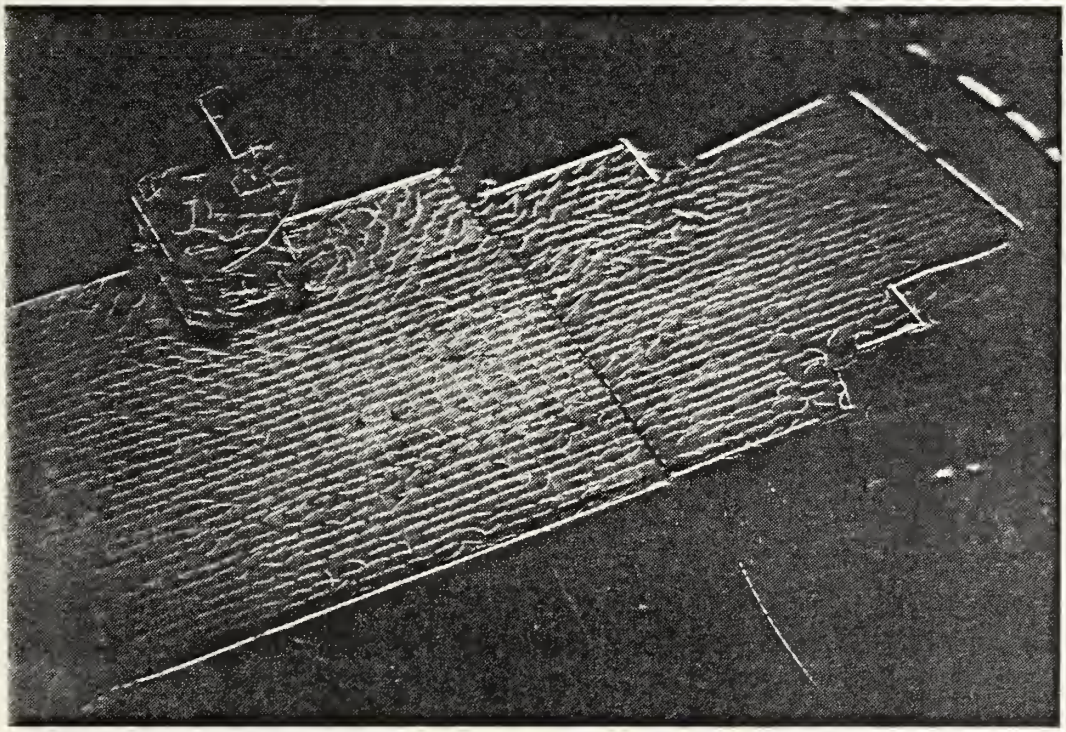

(b) Fluorescent Minituft

Figure 17. Aft: 0^{o} Yaw, Oscillating Pitch and Roll

and 2 on the bow and the influence that the shear flow would have, flapping the main rotor blades. When the model oscillates, the bubble traces reveal interesting activity in the vicinity of spot 3 on the angled deck. Fluid particle paths, generated at the point where the leading edge of the angled deck meets the bow, propagate down the deck for some distance (Figure 28a). An argument can be made that spot 3 should be moved inboard so as to avoid, as much as possible, the shear flow coming up and over the port edge of the flight deck when winds are from the port side. However, as seen in Figure 28a, an inboard move would subject a helicopter to shear flow on its right side.

Photographs of the aft portion of the model are fairly similar. Bubble traces down the flight deck conform to the general direction of the oncoming free stream flow, although occasionally pathlines traced from the port deck edge (Figures 19a, 21a, 23a and 27a) and from the leading edge of the angled deck (Figure 27a) are seen to be crossing the general flow at an angle. This activity persists along the remaining length of the model and the pathlines in question never appear to merge with those that follow the dominant direction of flow.

The fluorescent minituft photographs once again served to confirm that the flow across the flight deck was generally of low turbulence level. The photographs were all time-elapsed shots except for those taken when the model was

oscillating (Figures 28b and 29b). The separation detected in the helium bubble photographs of the bow was not evident in the minituft prints, thereby confirming Crowder's observation [Ref. 15:p. 55], discussed in Chapter III, that small separation regions may go undetected. The only significant activity observed was around the superstructure, where the changing direction of the minitufts conformed to the pattern typical of a horseshoe vortex as it wraps around a bluff body. The presence of air wake turbulence further aft on the model was absent, thereby indicating that the vortices had been blown off the starboard deck edge, just behind the superstructure.

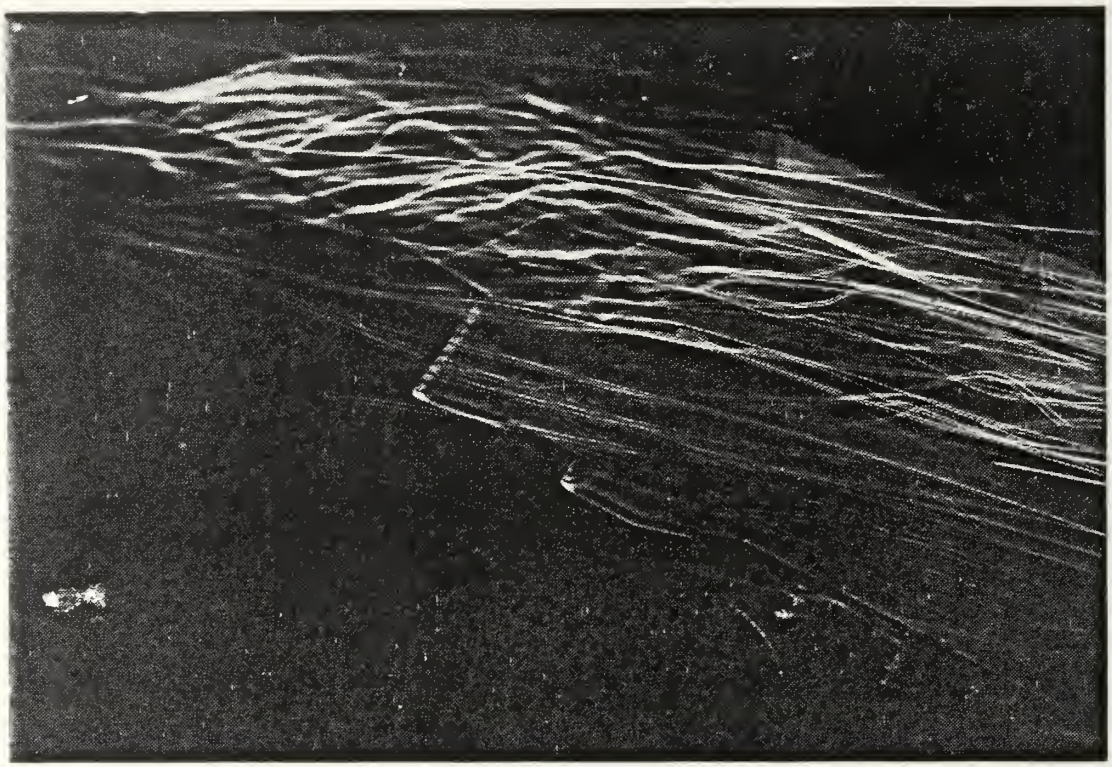

(a) Helium Bubble

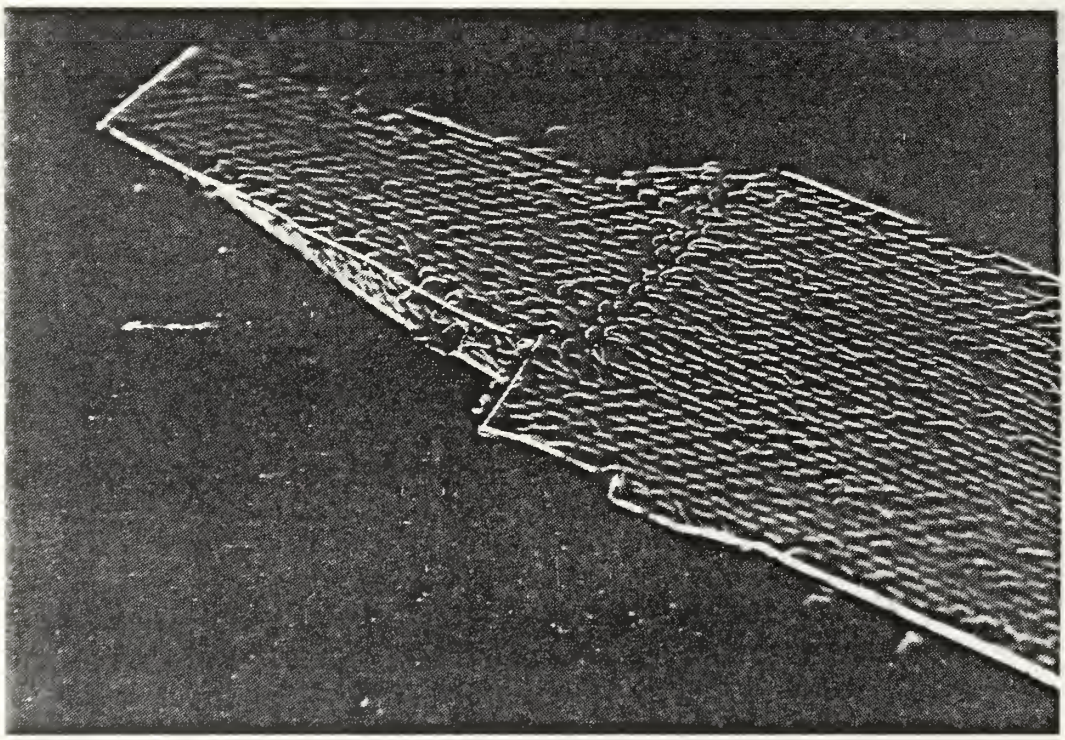

(b) Fluorescent Minituft

Figure 18. Forward: 12° Yaw, 0° Pitch, 0° Roll

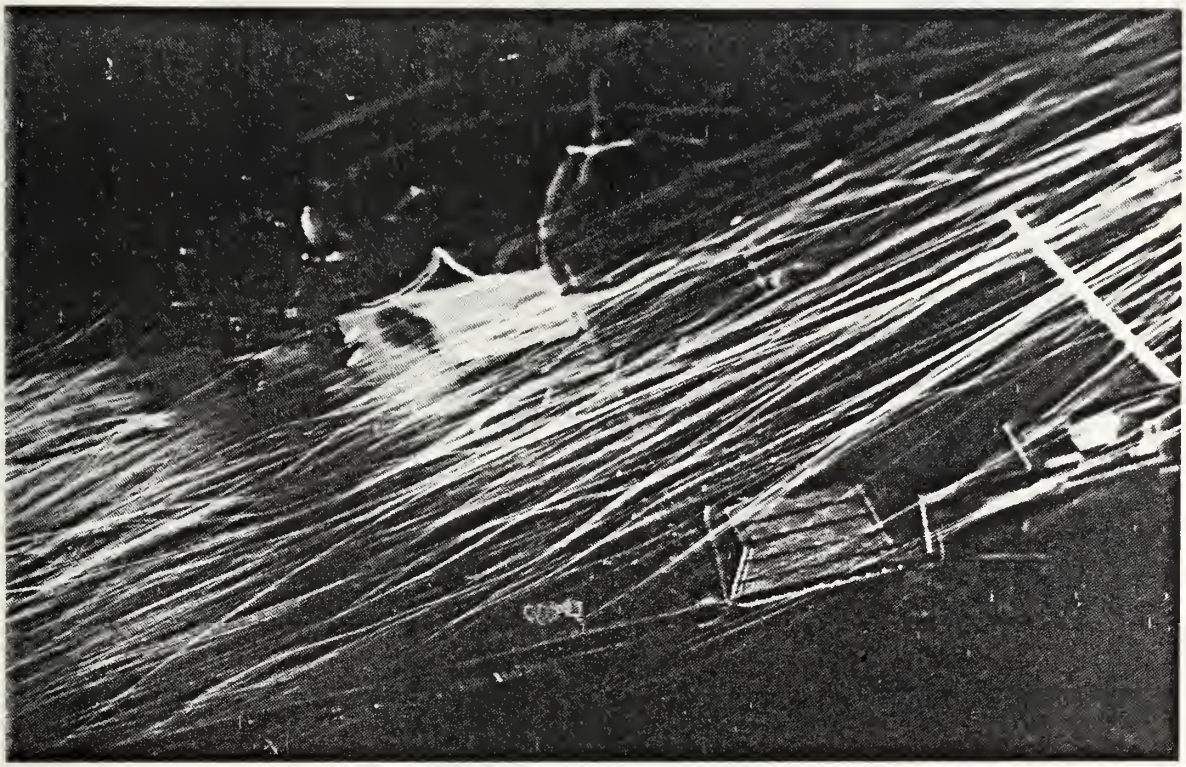

(a) Helium Bubble

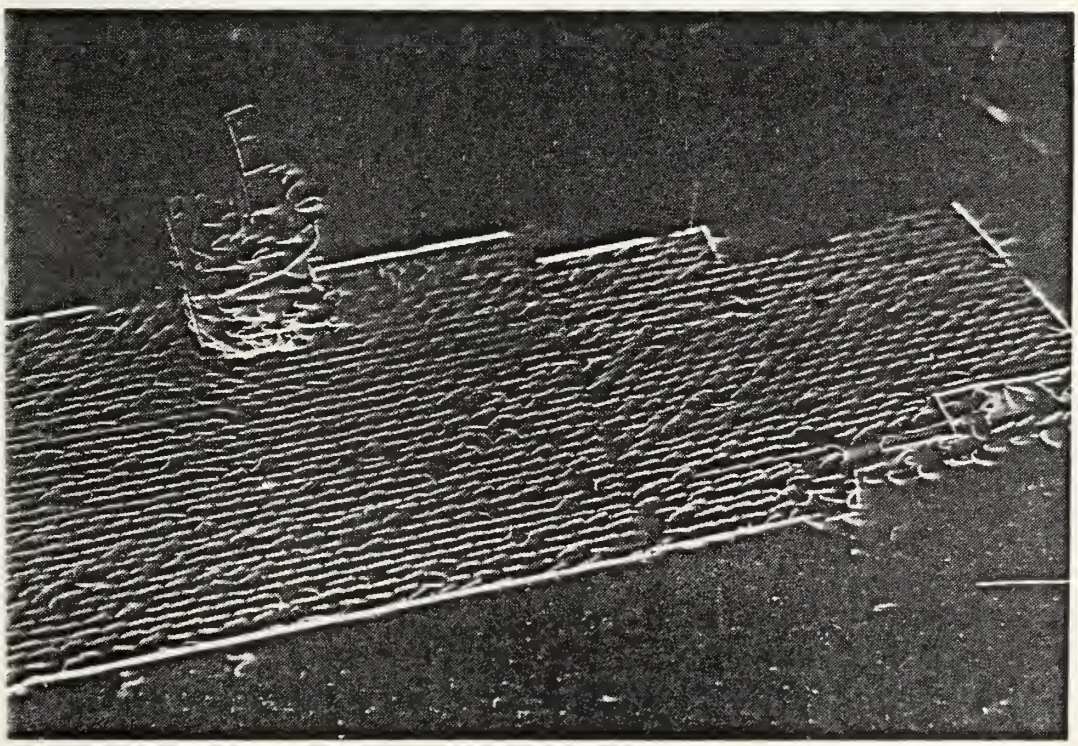

(b) Fluorescent Minituft

Figure 19. Aft: 12° Yaw, 0° Pitch, 0° Roll

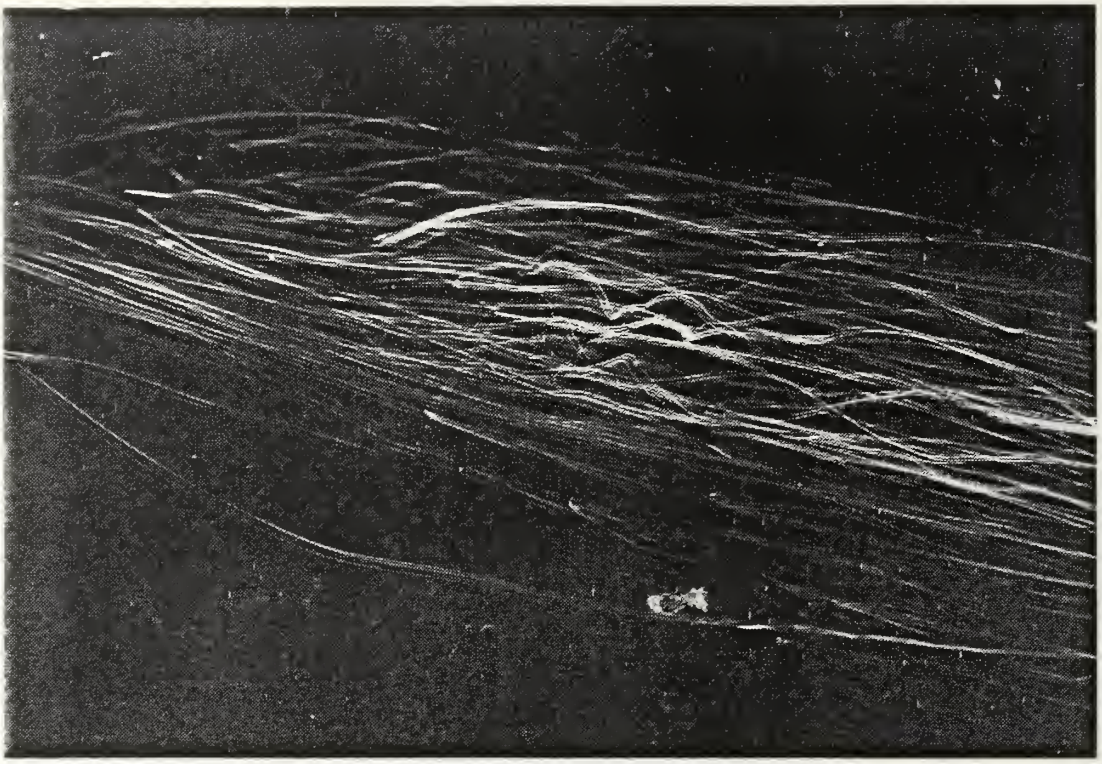

(a) Helium Bubble

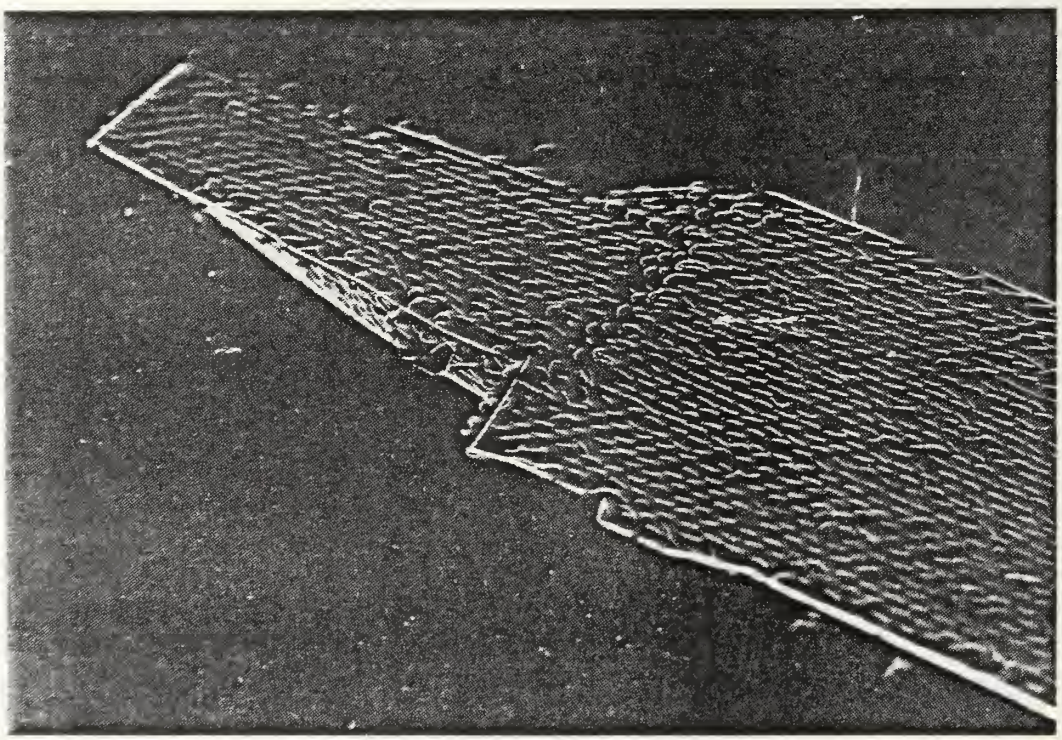

(b) Fluorescent Minituft

Figure 20. Forward: 12° Yaw, 1.25° Up Pitch, 0° Roll

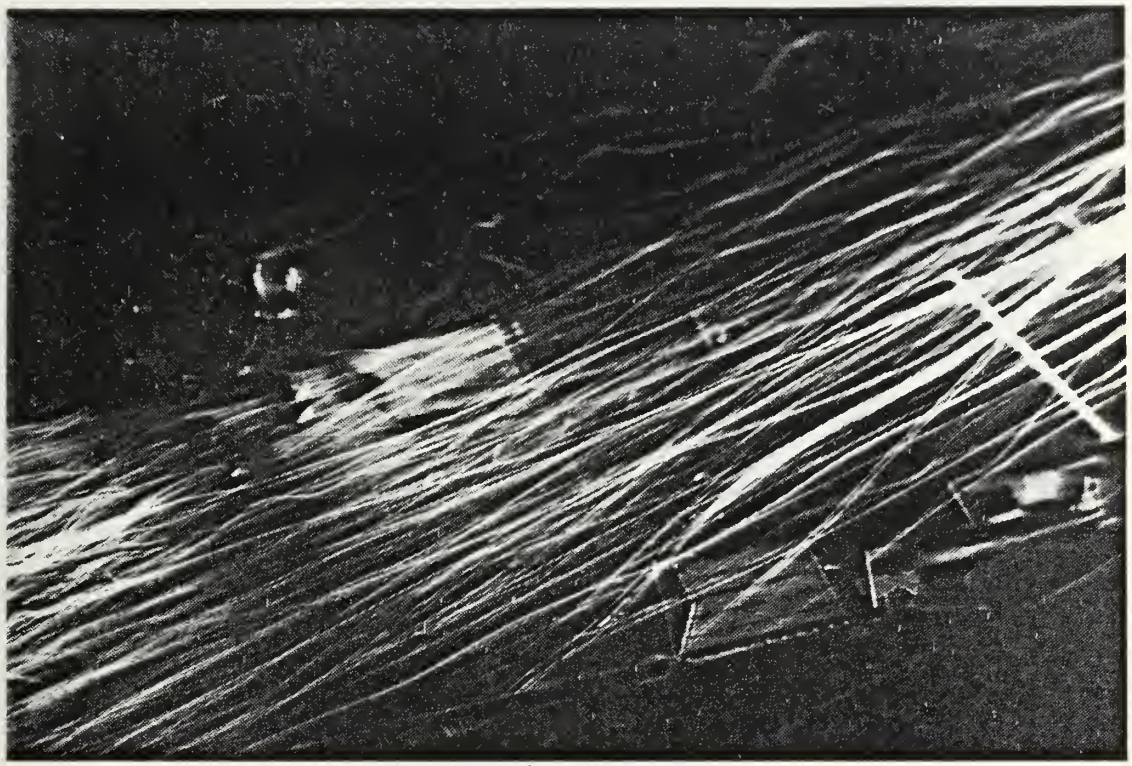

(a) Helium Bubble

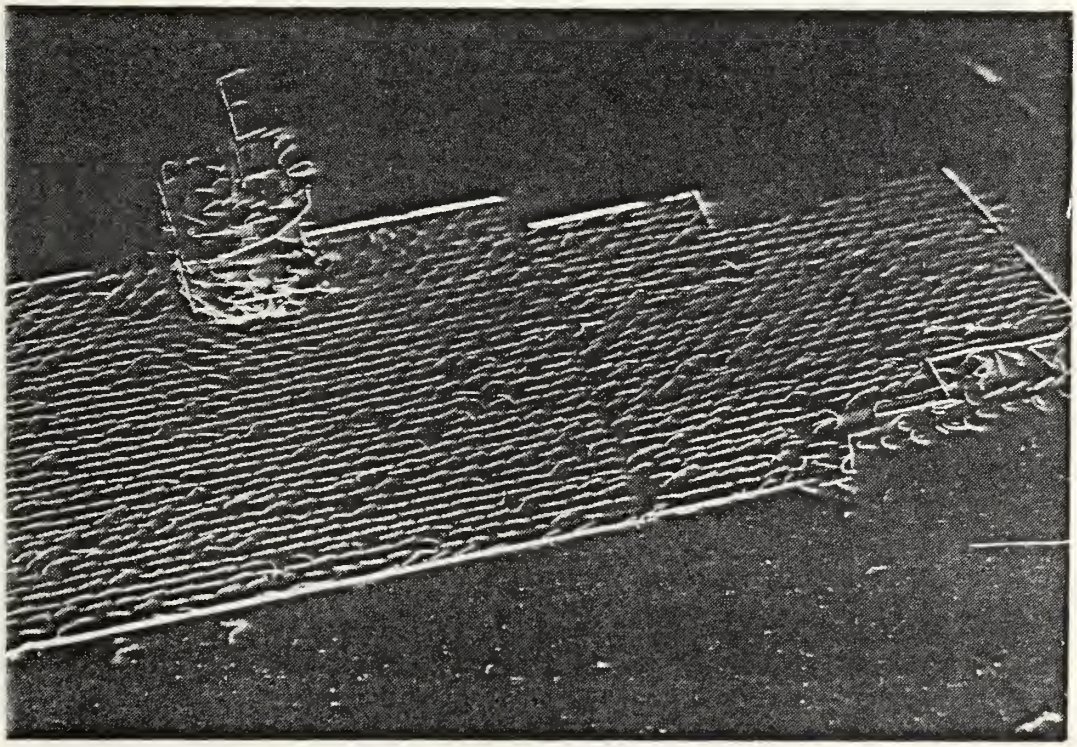

(b) Fluorescent Minituft

Figure 21. Aft: 12° Yaw, 1.25° Up Pitch, 0° Roll

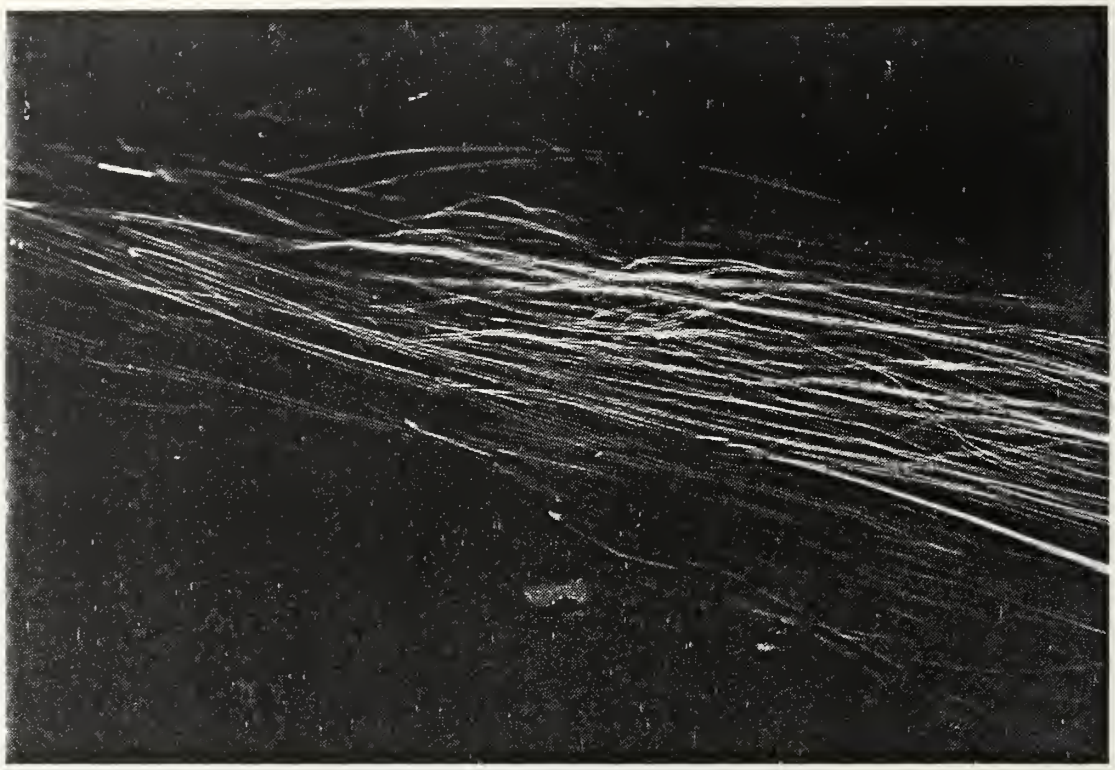

(a) Helium Bubble

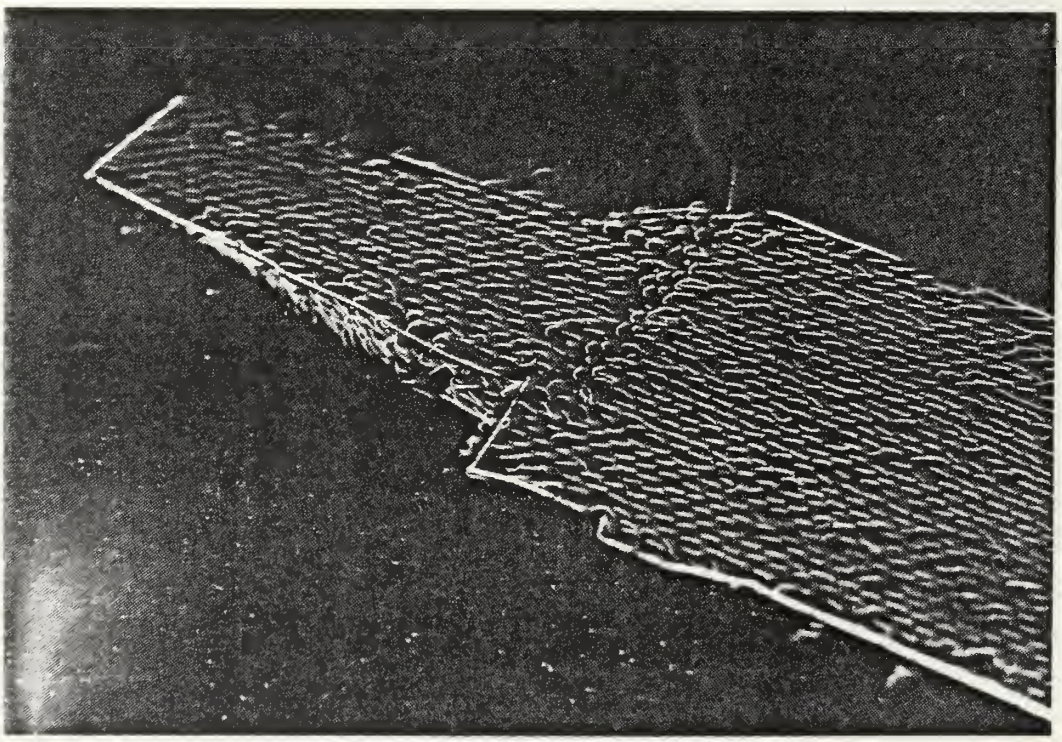

(b) Fluorescent Minituft

Figure 22. Forward: 12° Yaw, 1.25° Down Pitch, 0° Roll

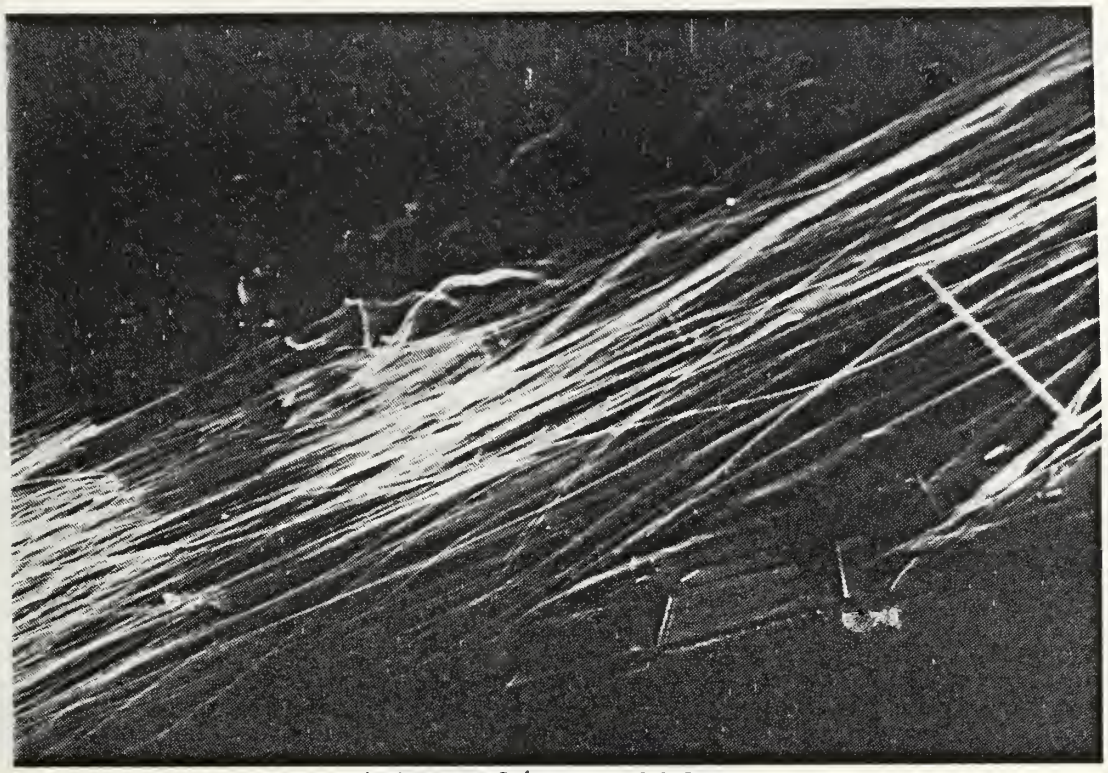

(a) Helium Bubble

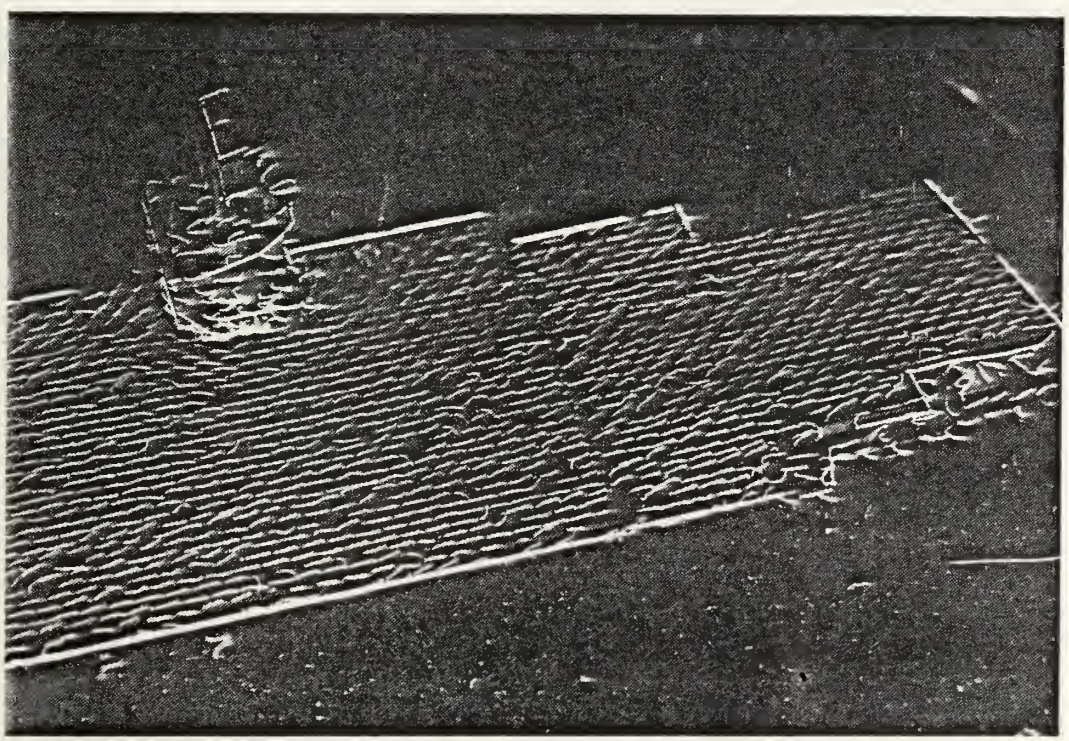

(b) Fluorescent Minituft

Figure 23. Aft: 12° Yaw, 1.25° Down Pitch, 0° Roll

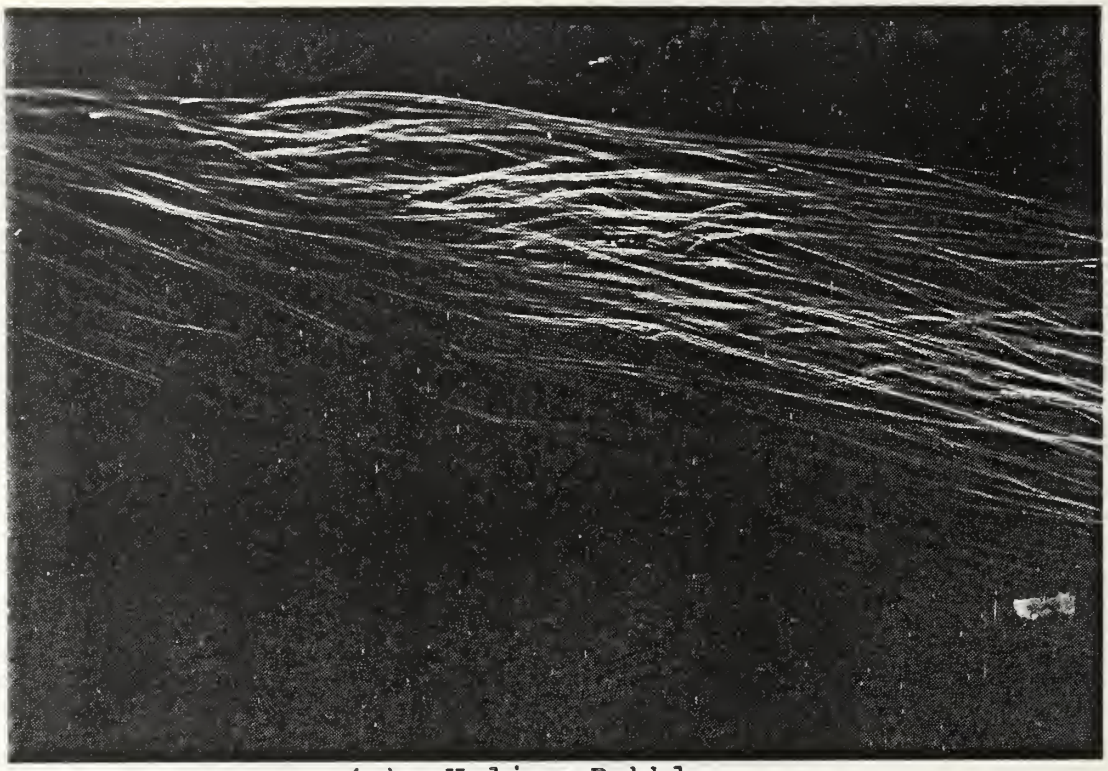

(a) Helium Bubble

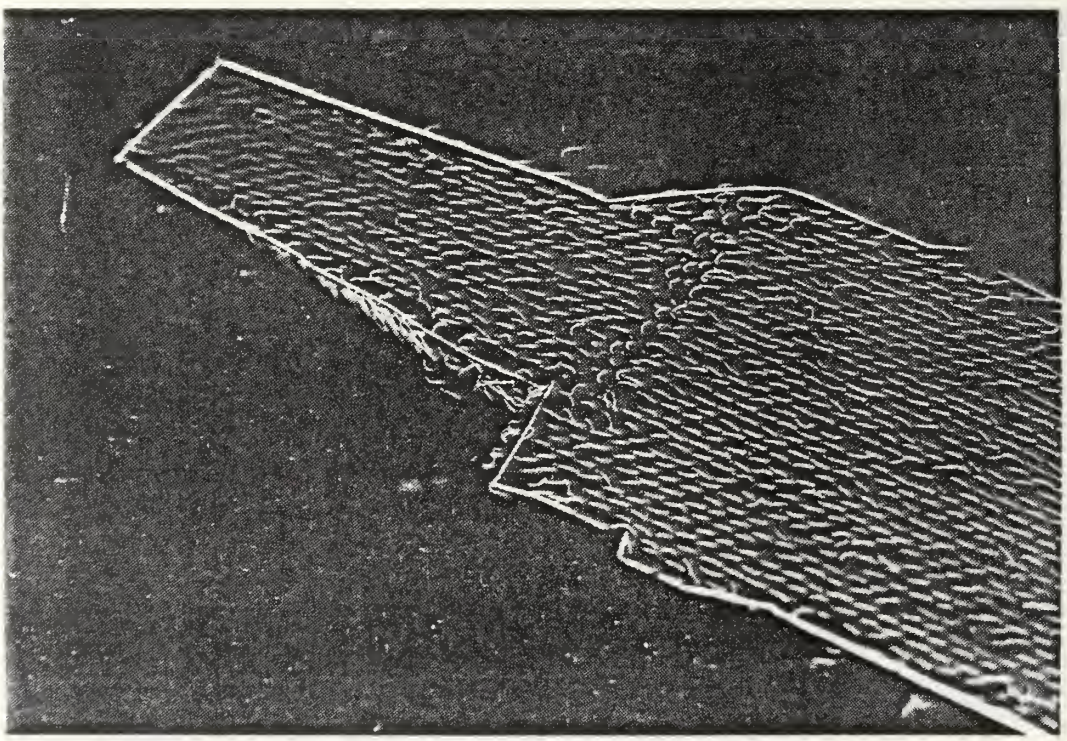

(b) Fluorescent Minituft

Figure 24. Forward: 12° Yaw, 0° Pitch, 6° Port Roll

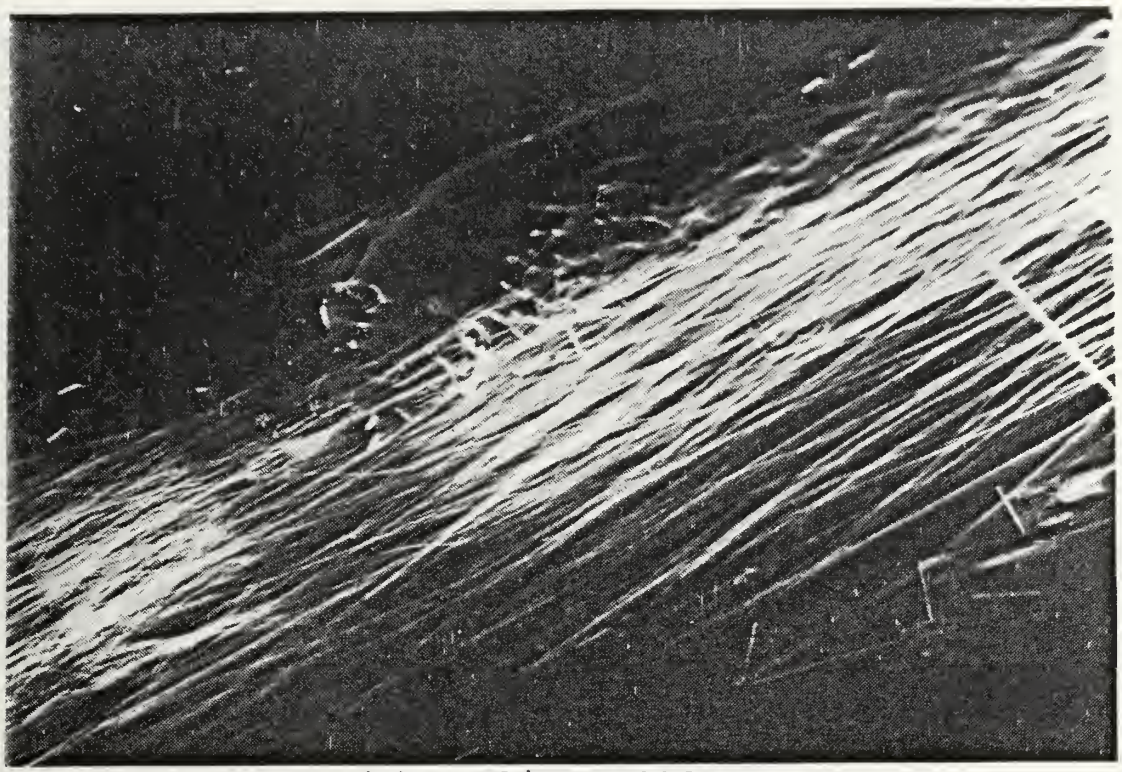

(a) Helium Bubble

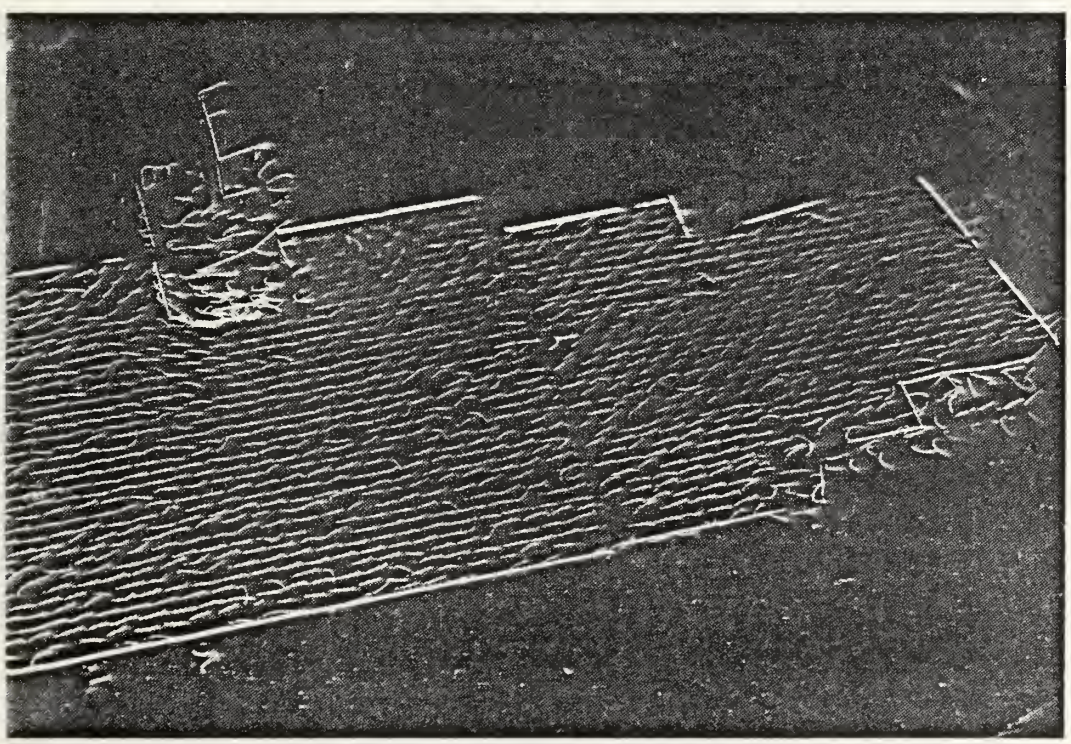

(b) Fluorescent Minituft

Figure 25. Aft: 12° Yaw, 0° Pitch, 6° Port Roll

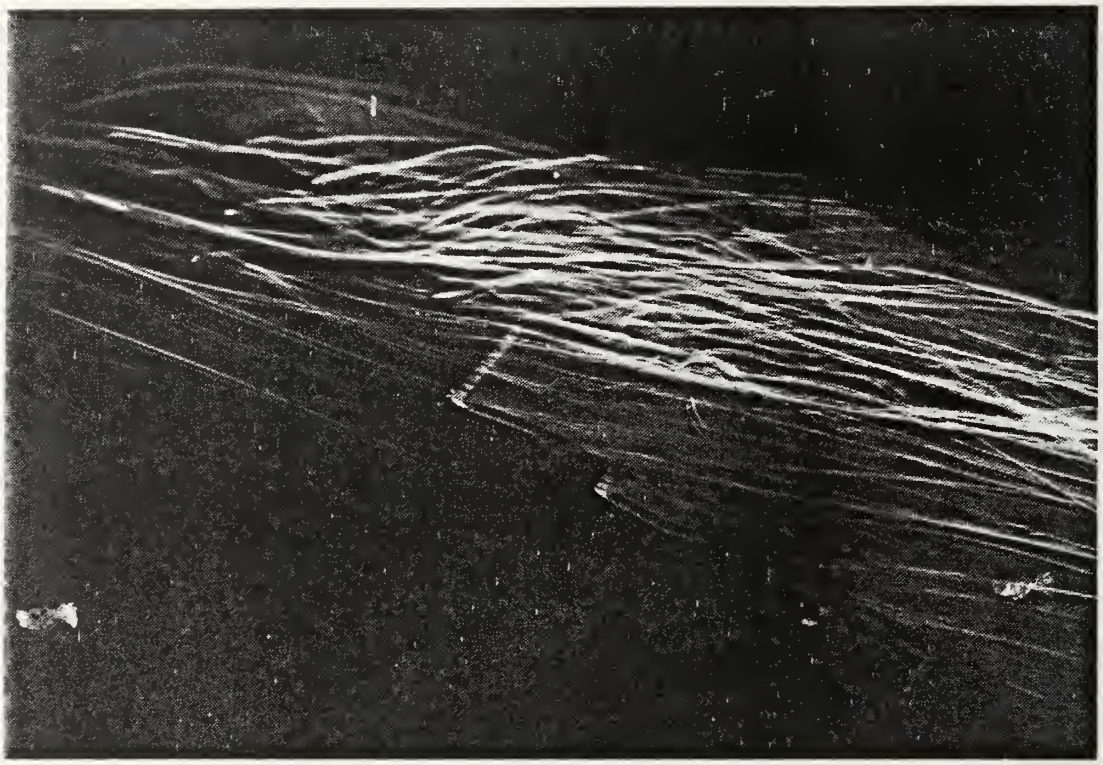

(a) Helium Bubble

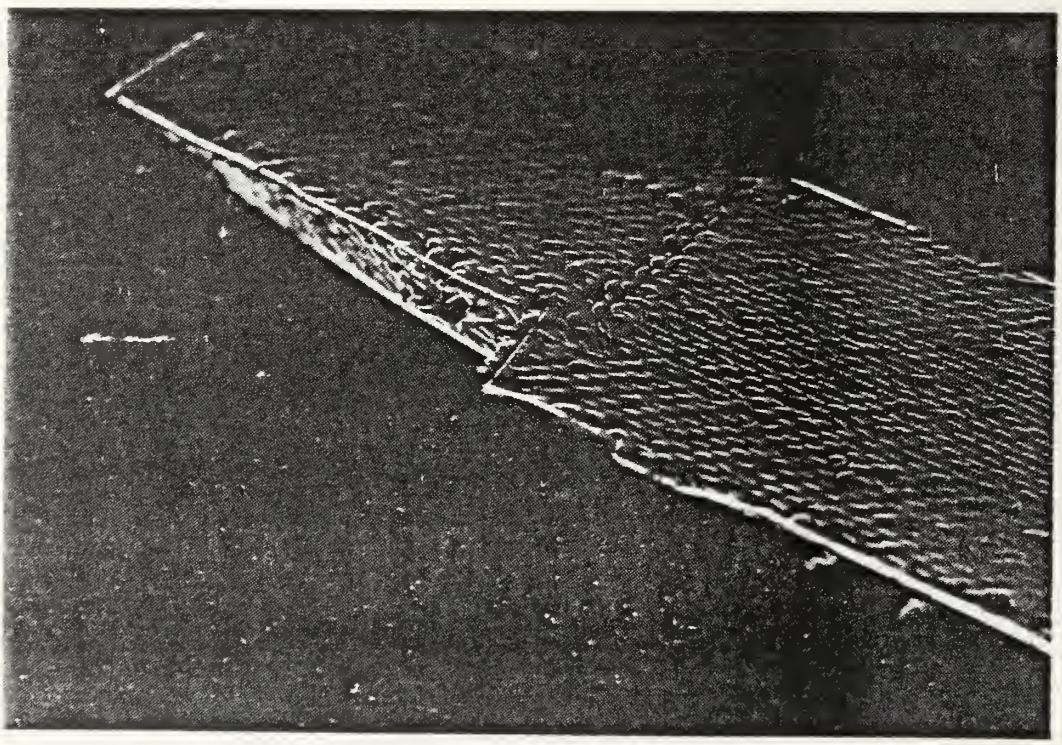

(b) Fluorescent Minituft

Figure 26. Forward: 12° Yaw, 0° Pitch, 6° Starboard Roll

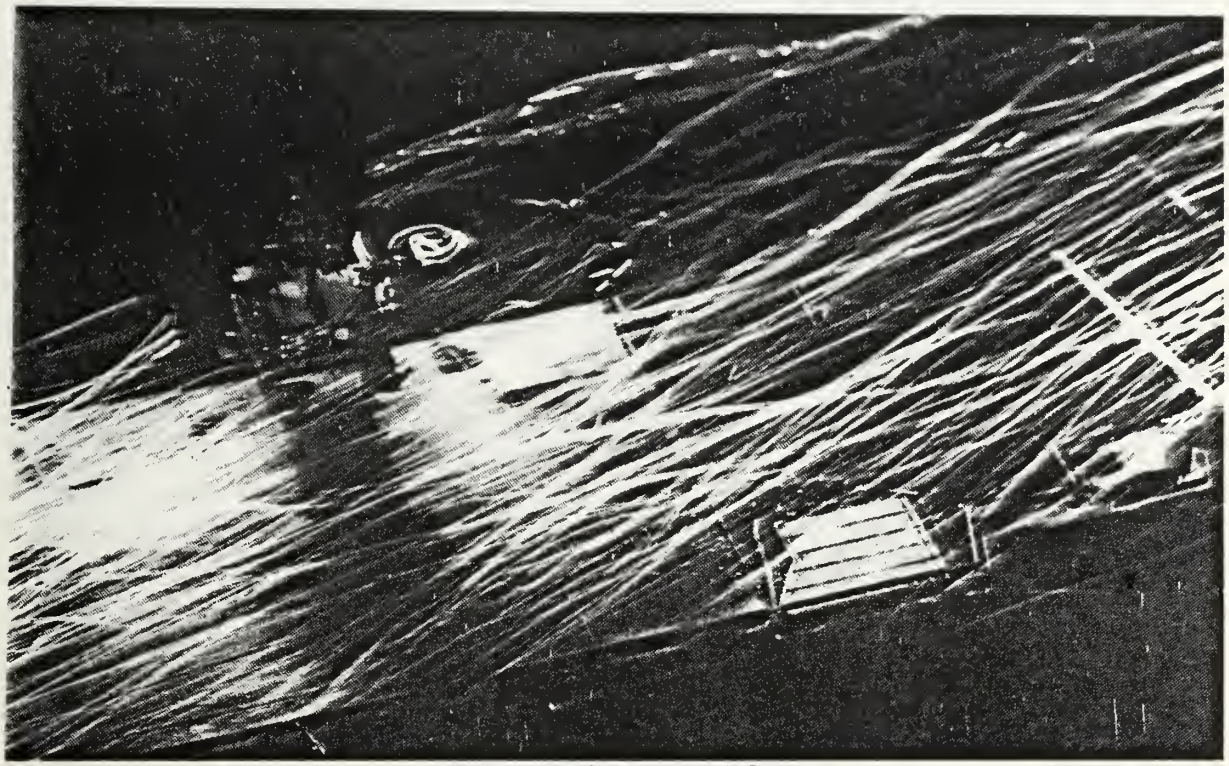

(a) Helium Bubble

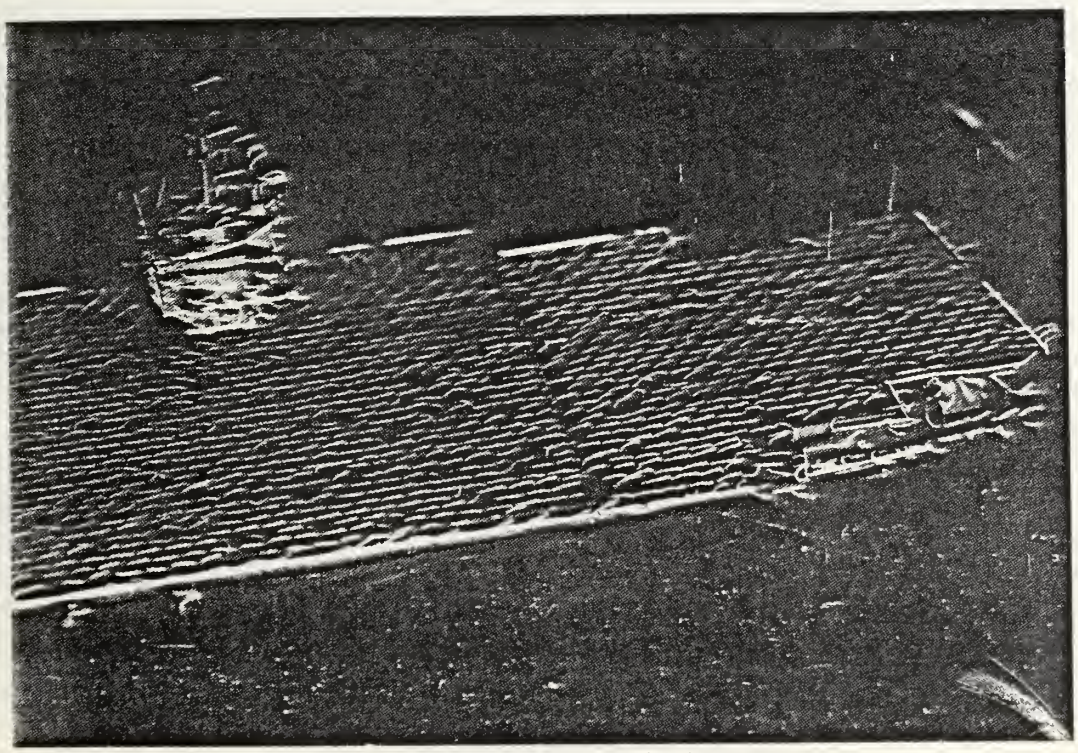

(b) Fluorescent Minituft

Figure 27. Aft: 12° Yaw, 0° Pitch, 6° Starboard Roll

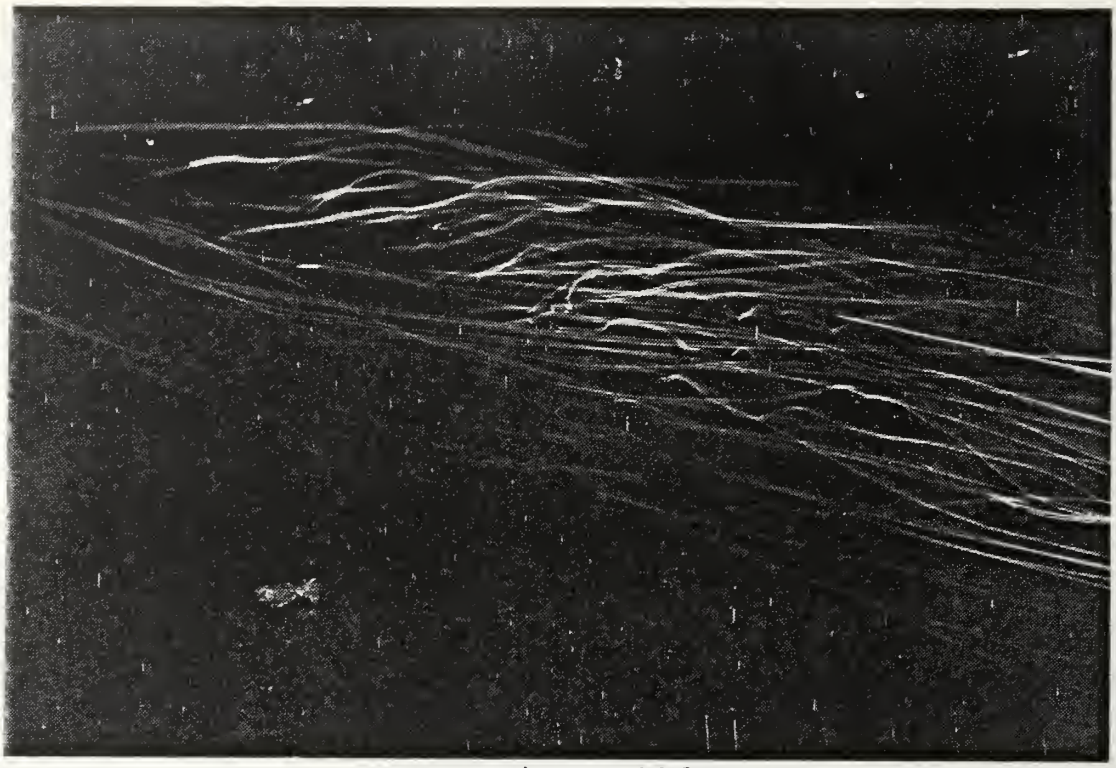

(a) Helium Bubble

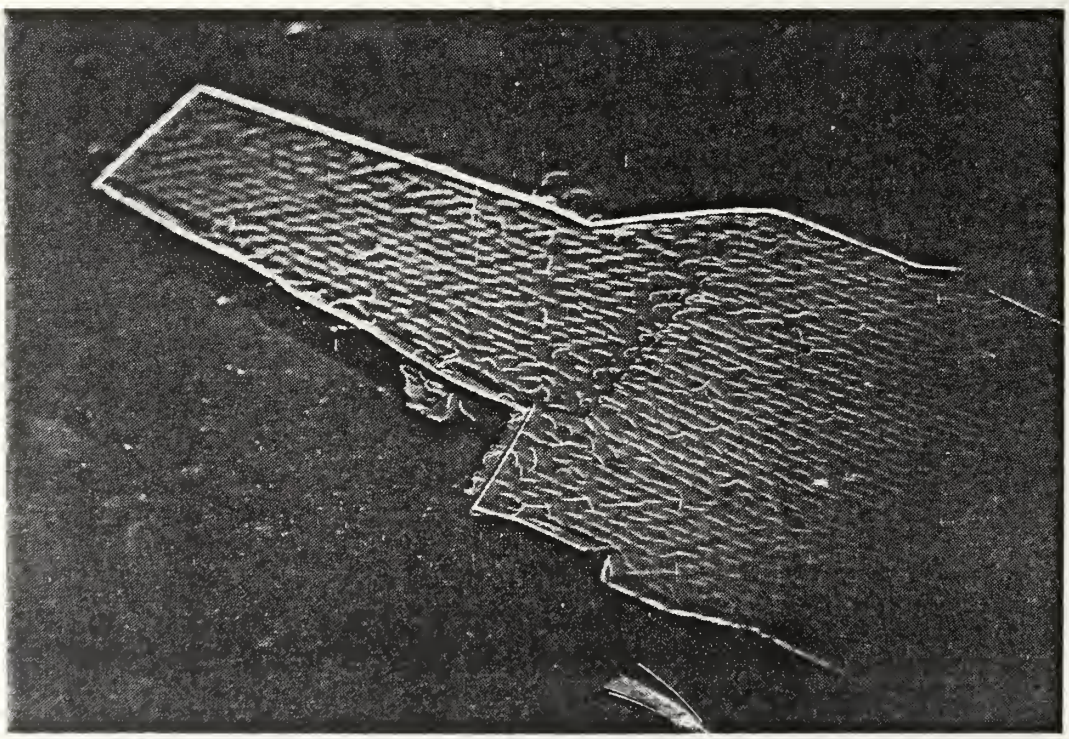

(b) Fluorescent Minituft

Figure 28. Forward: 12^{o} Yaw, Oscillating Pitch and Roll

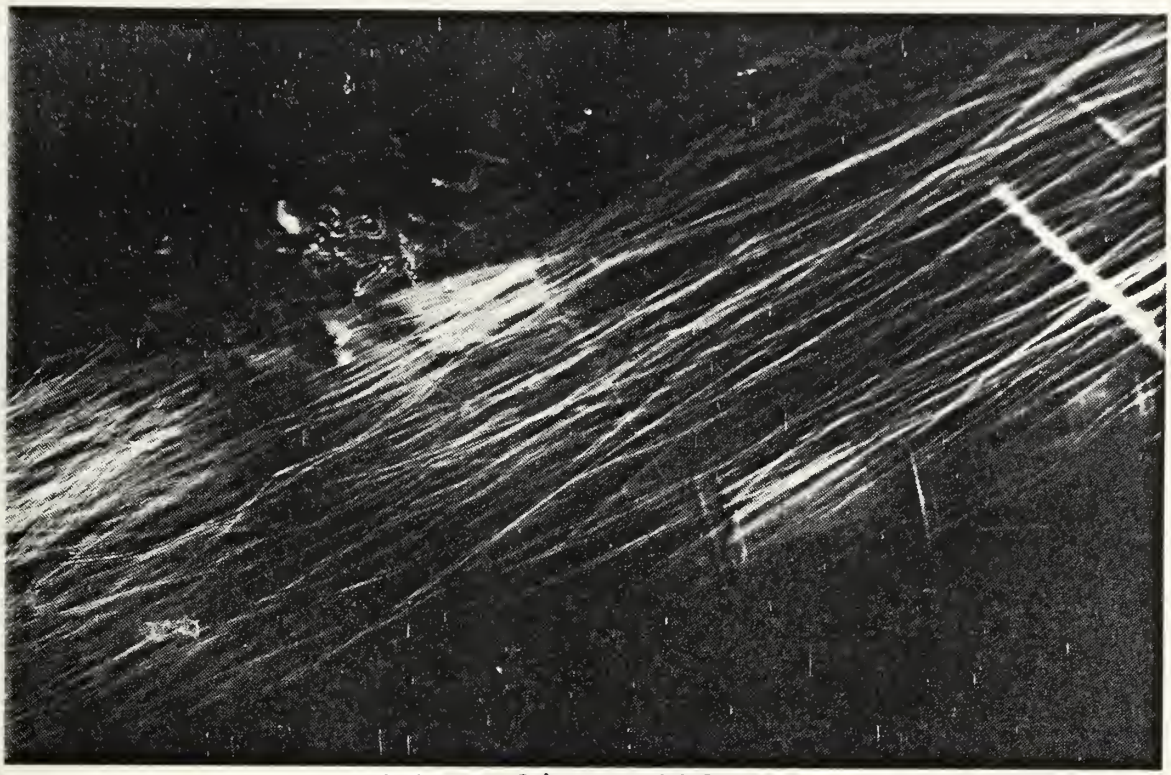

(a) Helium Bubble

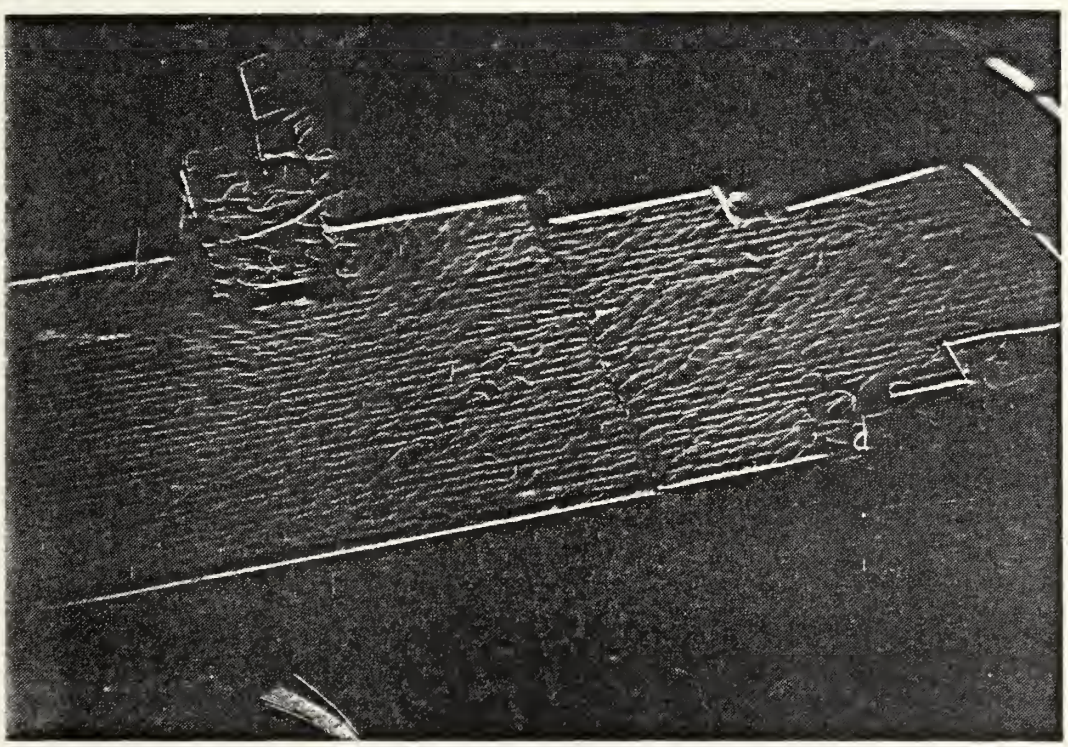

(b) Fluorescent Minituft

Figure 29. Aft: 12° Yaw, Oscillating Pitch and Roll

V. CONCLUSIONS AND RECOMMENDATIONS

This report summarizes the theories, procedures and techniques employed in conducting a flow visualization study of an oscillating 1:350 scale model of the USS Enterprise (CVN-65) in a simulated atmospheric boundary layer. Several conclusions are drawn and recommendations are offered.

A. HELIUM BUBBLE FLOW VISUALIZATION

This technique produced excellent results. Despite the small scale of the model, subtle changes to the flow were perceptible when the model was pitched and rolled. When the model was rolled to the leeward side (away from the free stream flow), the presentation of a greater surface area to the wind increased the wake size and turbulence level. Aircraft carrier conning officers follow a "30 rule"; the speed of the ship in knots plus the number of degrees of rudder should equal less than 30 when maneuvering the ship. This rule is followed so as to minimize ship roll and the effects that roll has on flight deck operations. This helium bubble study supports continued adherence to this rule. Turning the ship while a helicopter is engaging/disengaging its main rotor blades may lead to an adverse increase in shear force on the blades.

Additional yaw angle settings need to be investigated with this model. A 360^{o} swing in 30^{o} increments, is

appropriate for this aircraft carrier model and for any other dedicated, aviation support ship (LHA, LHD, LPD). The swing should be conducted with the ship model level (0^{o} pitch, 0^{o} roll) or, if additional arc lamps are purchased, oscillating, so long as the lighting is bright enough to capture one cycle of motion as nearly as possible.

As the model is yawed, it presents an increasingly larger profile to the free stream wind. The helium bubble coverage correspondingly needs to be expanded. The employment of a newly acquired helium bubble system simultaneously with the existing system will assist in mapping the air wake. Acquisition of a high resolution video recording system would also aid in analysis and record keeping.

B. FLUORESCENT MINITUFT TECHNIQUE

The minitufts uncovered a large area of separation around the superstructure, but otherwise conformed to the dominant flow direction. Ship models that possess large flat areas and little superstructure development (CV, LHA, LHD, LPH) need not be fully tufted to obtain meaningful information. On the other hand, the analysis of ships with significant superstructure development (DD, FF, LST, LSD, etc.) would benefit from complete minituft coverage.

Two of the four ballasts that form the bank of UV fluorescent light tubes below the observation window are inoperative and in need of repair. In the event that the

observation window is replaced and lowered, room should remain to accommodate one ballast to provide lateral UV lighting. To increase UV lighting and improve depth of field, aluminum foil should be spread behind the existing tubes. An overhead bank of UV fluorescent tubes should be installed on the tunnel ceiling. Additionally, acquisition of another Norman lamp head, to be mounted low in the tunnel along with a UV transmitting filter, would help to illuminate the hull of the model when it undergoes oscillation. This improvement should be implemented when the planned expansion of the test section is completed, due to the bulk of the flash unit.

C. THESIS TOPIC SUGGESTION

A study should be undertaking to examine in detail how safe operating envelopes are determined. Past air wake studies of full scale and model fleet units should be collected, organized and studied. Previously conducted dynamic interface tests should also be obtained and reviewed so that an understanding is achieved of how they are conducted and what equipment and pilot rating scales are employed. A library of current safe operating envelopes, launch and recovery bulletins, and any other literature that would increase awareness of the manner in which flight operations are conducted at sea, and inclusion of the Naval Postgraduate School on appropriate distribution list, would be of value to future air wake mapping investigations. A

study of this type would help to focus the attention of wind tunnel investigators, who are principally concerned with the establishment of an accurate simulation, on matters relevant to flight test and fleet needs.

LIST OF REFERENCES

1. Carico, Dean, McCallum and Higman, "Dynamic Interface Flight Test and Simulation Limitations," Eleventh European Rotocraft Forum, Paper #100, September 1985, pp. 100-1, 100-19.

2. Healey, J. Val, "Simulating the Helicopter-Ship Interface as an Alternative to Current Methods of Determining the Safe Operating Envelopes," NPS Report NPS67-86-003, September 1986, Naval Postgraduate School, Monterey, CA 93943-5001.

3. Paulk, C.H. Jr., Astill, D.L. and Donley, S.T., "Simulation and Evaluation of the SH-2F Helicopter in a Shipboard Environment Using the Interchangeable Cab System," NASA TM-84387, August 1983, p. 87.

4. Rae, W.H. Jr. and Pope, A., Low Speed Wind Tunnel Testing, 2d ed., John Wiley and Sons, Inc., New York, 1984.

5. Davenport, A.G., in Engineering Meteorology, E.J. Plate, Editor, Elsevier Scientific Publishing Company, Amsterdam, Netherlands, 1982, Chapter 12, pp. 527, 569.

6. Garratt, J.R., "Review of Drag Coefficients over Oceans and Continents," Monthly Weather Review, July 1977, pp. 915, 929.

7. E.S.D.U. Data Items 74030, 74031, Engineering Science Data Unit International, Suite 200, Chain Bridge Road, McLean, VA 22101.

8. Bolinger, W.K., Visualization of the Flow Field Around a Generic Destroyer Model in a Simulated Turbulent Atmospheric Boundary Layer, Master's Thesis, Naval Postgraduate School, Monterey, CA, June 1987.

9. Counihan, J., "An Improved Method of Simulating An Atmospheric Boundary Layer in a Wind Tunnel," Atmospheric Environment, Vol. 3, pp. 197-214, 1969.

10. Biskaduros, J. L., Flow Visualization of the Airwake of an Oscillating Generic Ship Model. Master's Thesis, Naval Postgraduate School, Monterey, CA, December 1987.

11. Bowditch, N., American Practical Navigator, H. O. Pub. No. 9, U. S. Government Printing Office, Washington, DC, 1966, p. 1059.

12. Meyers, W.G., Applebee, T.R. and Baitis, A.E., "User's Manual for the Standard Ship Motion Program, SMP," DTNSRDC/SPD-0936-01, September 1981.

13. Meyers, W.G. and Baitis, A.E., "SMP84: Improvements to Capabilities and Prediction Accuracy of the Standard Ship Motion Program SMP81," DTNSRDC/SPD-0936-04, September 1985.

14. Mueller, T.J., "Flow Visualization by Direct Injection," in Fluid Mechanics Measurements, ed. Richard J. Goldstein. Washington: Hemisphere Publishing Co., 1983.

15 Crowder, J.P., "Add Fluorescent Minitufts to the Aerodynamicists Bag of Tricks," Astronautics and Aeronautics, November 1980, pp. 54-57.

INITIAL DISTRIBUTION LIST

		No. Copies
1.	Defense Technical Information Center Cameron Station Alexandria, VA 22304-6145	2
2.	Library, Code 0142 Naval Postgraduate School Monterey, CA 93943-5002	2
3.	Department Chairman, Code 67 Department of Aeronautics and Astronautics Naval Postgraduate School Monterey, CA 93943	1
4.	Commander Naval Air Systems Command Air Vehicle Division Attn: Mr. Jonah Ottensoser, Code Air 53011C Jefferson Plaza 2, Rm. 904 Washington, DC 20361	1
5.	David Taylor Naval Ship Research and Development Center Attn: Eric Baitis, Code 1561 Bethesda, MD 20084	1
6.	Naval Research Laboratory Atmospheric Physics Division Attn: Mr. Ted Blanc, Code 4110 Washington, DC 20375	1
7.	Naval Air Test Center Attn: Mr. Dean Carico, Code RW40A Patuxent River, MD 20670	1
8.	Naval Air Test Center Attn: Mr. Jerry Higman, Code RW81 Patuxent River, MD 20670	1
9.	Dr. J. Val Healey, Code 67He Department of Aeronautics and Astronautics Naval Postgraduate School Monterey, CA 93943	6

10. LT John L. Biskaduros, USN — 1
1301 Parkside Place
Virginia Beach, VA 23454

11. Mr. R.A. Feik — 1
Aeronautical Division
Aeronautical Research Laboratories
506 Lorimer Street
Fisherman's Bend
Box 4331 P.O.
Melbourne, Victoria 3001
Australia

12. LCDR Thomas A. Cahill, USN — 2
ASD/SDMN
Wright-Patterson AFB, OH 45433-6503

Thesis
C176 Cahill
c.1 Visualization of the flow field around an oscillating model of the USS Enterprise (CVN-65) in a simulated atmospheric boundary layer.